Potent and selective aldo-keto reductase 1C3 (AKR1C3) inhibitors based on the benzoisoxazole moiety: Application of a bioisosteric scaffold hopping approach to flufenamic acid

UNIVERSITÀ DEGLI STUDI DI TORINO

Potent and selective Aldo-Keto Reductase 1C3 (AKR1C3) inhibitors based on the benzoisoxazole moiety: Application of a Bioisosteric Scaffold Hopping Approach to Flufenamic acid

Agnese Chiara Pippione,[1] Irene Maria Carnovale,[1] Davide Bonanni,[1] Marcella Sini,[2] Parveen Goyal,[4] Elisabetta Marini,[1] Klaus Pors,[2] Salvatore Adinolfi,[1] Daniele Zonari,[1] Claudio Festuccia,[3] Weixiao Yuan Wahlgren,[4] Rosmarie Friemann,[4] Renzo Bagnati,[5] Donatella Boschi,[1] Simonetta Oliaro-Bosso[1]* and Marco Lucio Lolli[1]*

[1] *Department of Science and Drug Technology*, University of Torino, via Pietro Giuria 9, 10125 Torino (Italy).
[2] *Institute of Cancer Therapeutics*, School of Pharmacy and Medical Sciences, Faculty of Life Sciences, University of Bradford, BD7 1DP West Yorkshire (UK).
[3] *Department of Biotechnological and Applied Clinical Sciences*, Laboratory of Radiation Biology, University of L'Aquila, via Vetoio snc, Coppito II, 67100 L'Aquila (Italy).
[4] *Department of Chemistry and Molecular Biology*, University of Gothenburg, Box 462, S-40530 Gothenburg (Sweden).
[5] *IRCCS Istituto di Ricerche Farmacologiche Mario Negri*, Via La Masa 19, 20156 Milano (Italy).

Keywords
aldo-keto reductase 1C3; AKR1C3; 17β-HSD5; Prostate cancer (PCa); CRPC; bioisosterism; scaffold hopping; inhibitors; X-ray crystallography.

Abstract

The aldo-keto reductase 1C3 (AKR1C3) isoform plays a vital role in the biosynthesis of androgens and is considered an attractive target in prostate cancer (PCa). No AKR1C3-targeted agent has to date been approved for clinical use. Flufenamic acid and indomethacine are non-steroidal anti-inflammatory drugs known to inhibit AKR1C3 in a non-selective manner as COX off-target effects are also observed. Recently, we employed a scaffold hopping approach to design a new class of potent and selective AKR1C3 inhibitors based on a *N*-substituted hydroxylated triazole pharmacophore. Following a similar strategy, we designed a new series focused around an acidic hydroxybenzoisoxazole moiety, which was rationalised to mimic the benzoic acid role in the flufenamic scaffold. Through iterative rounds of drug design, synthesis and biological evaluation, several compounds were discovered to target AKR1C3 in a selective manner. The most promising compound of the series (**6**) was found to be highly selective (up to 450-fold) for AKR1C3 over the 1C2 isoform with minimal COX1 and COX2 off-target effects. Other inhibitors were obtained modulating the best example of hydroxylated triazoles we previously presented. In cell-based assays, the most promising compounds of both series reduced the cell proliferation, prostate specific antigen (PSA) and testosterone production in AKR1C3-expressing 22RV1 prostate cancer cells and showed synergistic effect when assayed in combination with abiraterone and enzalutamide. Structure determination of AKR1C3 co-crystallised with one representative compound from each of the two series clearly identified both compounds in the androstenedione binding site, hence supporting the biochemical data.

1. Introduction

AKR1C3, or HSD17B5, is a soluble enzyme member of the aldo-ketoreductase family, which is highly expressed in testes and extragonadal tissues such as basal cells of the prostate, adrenals and liver.[1] It catalyses the NADPH dependent reduction of androstenedione (AD) to testosterone and, compared to other HSD17B isoforms, is the most abundant isoform with elevated levels found in agressive PCa, such as castration-resistant prostate cancer (CRPC).[2] AKR1C3 may provide a mechanism to divert traces of androgens that remain after androgen deprivation therapy (ADT) to the potent androgen receptor (AR) ligand 5α-dihydrotesterone (DHT).[3] Besides evidence that AR mutations, splice variants and increased copy number represent putative mechanisms of resistance to therapy,[4-7] AKR1C3 has also been discovered to play a role in resistance to pharmacological[6] and radiation[8] therapy. Potential clinical use of AKR1C3 inhibitors has been demonstrated as in the case of indomethacin, a potent but unselective AKR1C3 inhibitor able to circumvent resistance to both abiraterone (ABI) [9] and enzalutamide (ENZA) [10] (Figure 1). Although few recent studies indicate controversial observations about the *in vivo* effectiveness of AKR1C3-based therapies,[11-13] other studies advocate for AKR1C3 as a therapeutic target in PCa.[2, 4] Even if several lead compounds have emerged from AKR1C3-targeting medicinal chemistry programs,[14-17], no agent has been approved yet for clinical use.[18]

In order to understand the clinical potential of targeting AKR1C3, it is desirable to develop more potent, selective and drug-like AKR1C3 inhibitors. Amongst NSAIDs, flufenamic acid (FLU, Figure 1) inhibits AKR1C3 in a non-selective manner, as it suffers from cyclooxygenase (COX) off-target effects.[19, 20] The COX active site consists of a narrow long hydrophobic channel that ends with a charged arginine residue (Arg120), which provides a suitable pocket for a ligand that contains a carboxylate group.[21] The carboxylic acid moiety of all the fenamate inhibitors forms a salt bridge with Arg120, with the two carboxylate oxygen atoms of fenamates within the proximity of 1.45 Å and 1.60 Å from one of the guanidine nitrogens of the arginine. This binding mode affects the ionic bond enthalpies and impacts on the overall inhibitory effect.[21] Removal of this carboxylic acid moiety in fenamate derivatives concurs with reduction of COX1 activity as demonstrated by us in a recent report on the design of new AKR1C3 inhibitors.[22] We successfully applied a *scaffold hopping* strategy based on the replacement of the FLU benzoate moiety with three hydroxyazoles (hydroxyfurazan, hydroxythiadiazole and a series of *N*-substituted hydroxyl-1,2,3-triazoles). Through the design of these new ligands we showed that hydroxyazoles are valid bioisosters of the carboxylic acid function. Depending on their acidic properties, they can be deprotonated to various degrees at physiological pH.[23-26] Inside the series, we demonstrated how the replacement of the benzoic acid of FLU with a 4-hydroxy-N1-substituted triazolecarbonylic moiety enables a bioisosteric *scaffold-hopping* replacement for AKR1C3 activity with no associated COX effect. Moreover, regiosubstitution of nitrogen atoms of the hydroxytriazole ring allowed the possibility to perform a structural refinement,[27] which enabled an opportunity to improve AKR1C3 binding while reduce AKR1C2 and COX1/2 off-target binding.

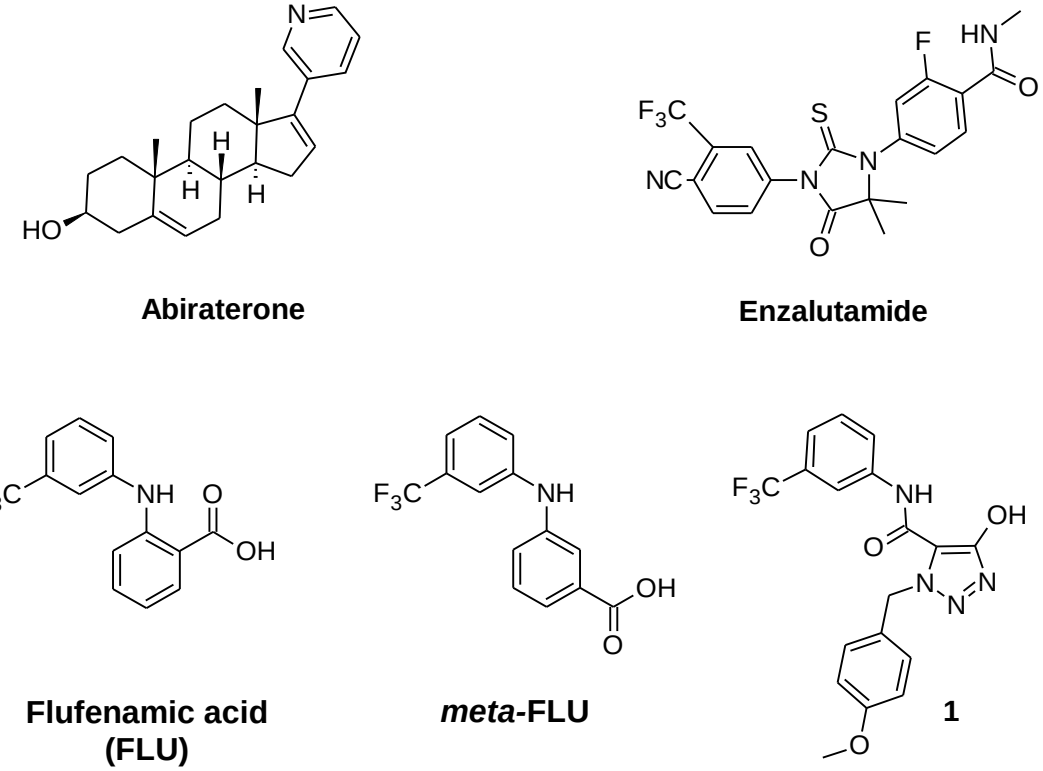

Figure 1. Chemical structures of some known AKR1C3 inhibitors.

Hydroxytriazole **1**[22] (Figure 1), the most active compound of our previous study, was used as starting point to design two triazoles **2** and **3** (Figure 2) bearing two *p*- and *m*-methoxy or one *p*-trifluoromethoxy substituents, respectively. In analogy to **1**, the rationale was to project its 4-methoxybenzyl moiety into the unexplored SP2 sub-pocket of AKR1C3 and thereby establishing, as the docking studies suggested, π-π staking and T-shape π-π staking with Trp227 (partial overlapping) and Trp86[22]; the new substitutions in the phenyl ring provided an opportunity to reinforce the binding by establishing interactions with the polar Ser129 present in this pocket [22]. In the following, a conformational restriction approach was employed to improve the potency and the selectivity of FLU, resulting in the design of a small, but focused library of 3-hydroxybenzoxazole-based compounds in which the carboxylic acid substituent was fused with the benzene ring, in order to constrain one of FLU conformations (compounds **4** - **8**, Figure 2). We report here on synthetic strategies, biochemical and cell-based studies of the new compounds alone or in combination with ABI and ENZA. In addition, to demonstrate selective AKR1C3 inhibition with impact on testosterone and PSA synthesis, we also show the binding mode of compound **1** and the most potent 3-hydroxybenzoxazole (compound **6**) by high-resolution crystal structures of AKR1C3 complexed with each of these two compounds.

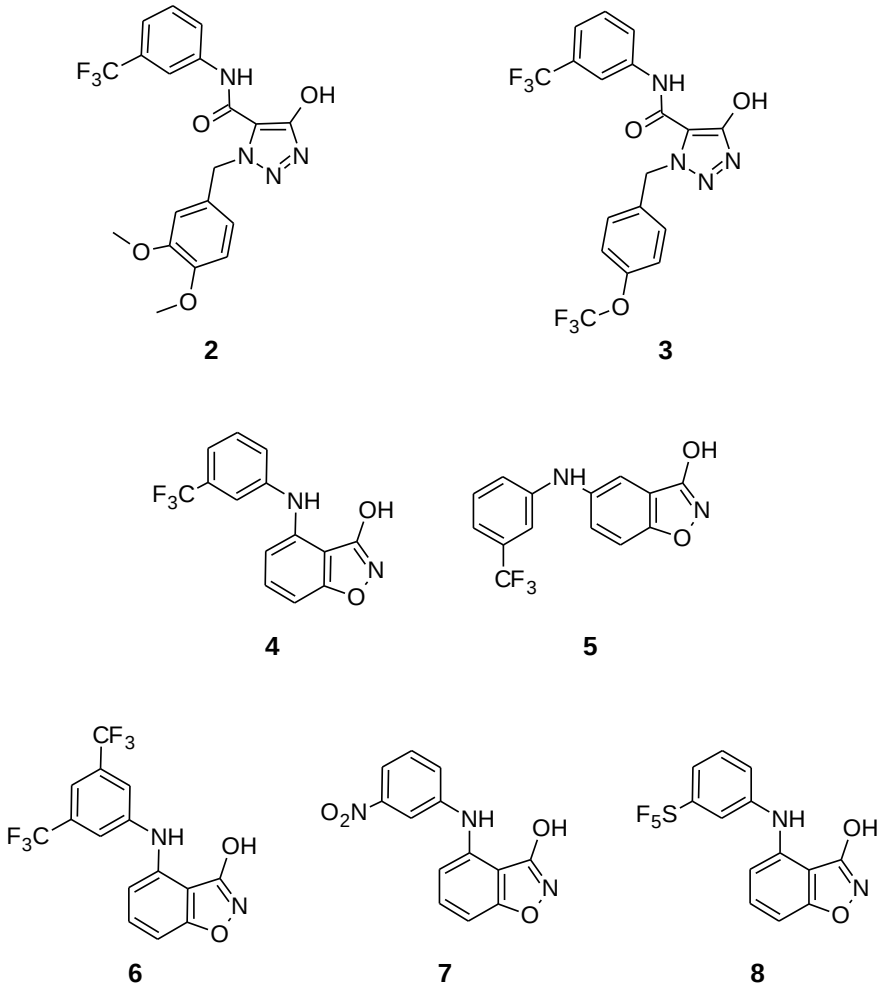

Figure 2. Chemical structures of AKR1C3 inhibitors studied in this work.

2. Result and discussion

2.1 Chemistry.

The methodology used for the synthesis of the two triazole derivatives **2** and **3** is described in Scheme 1. The common intermediate **9** was regioselectively alkylated by the appropriate benzylhalide using the procedure previously described.[23] The building block **9** is susceptible to alkylation directed towards positions $N_{(b)}$ and $N_{(c)}$ of the triazole ring, leading in each case to a mixture of two isomeric products(**10** - **12** and **11** - **13**, respectively). The isomeric mixtures were chromatographically resolved and the $N_{(c)}$ esters **10** and **12** were hydrolysed to the corresponding carboxylic acids **14** and **15**. The latter two compounds were converted into the corresponding acyl chlorides and allowed to react with 3-(trifluoromethyl)aniline to afford amides **16** and **17**, which were subsequently deprotected through catalytic hydrogenation to obtain the desired target compounds **2** and **3**.

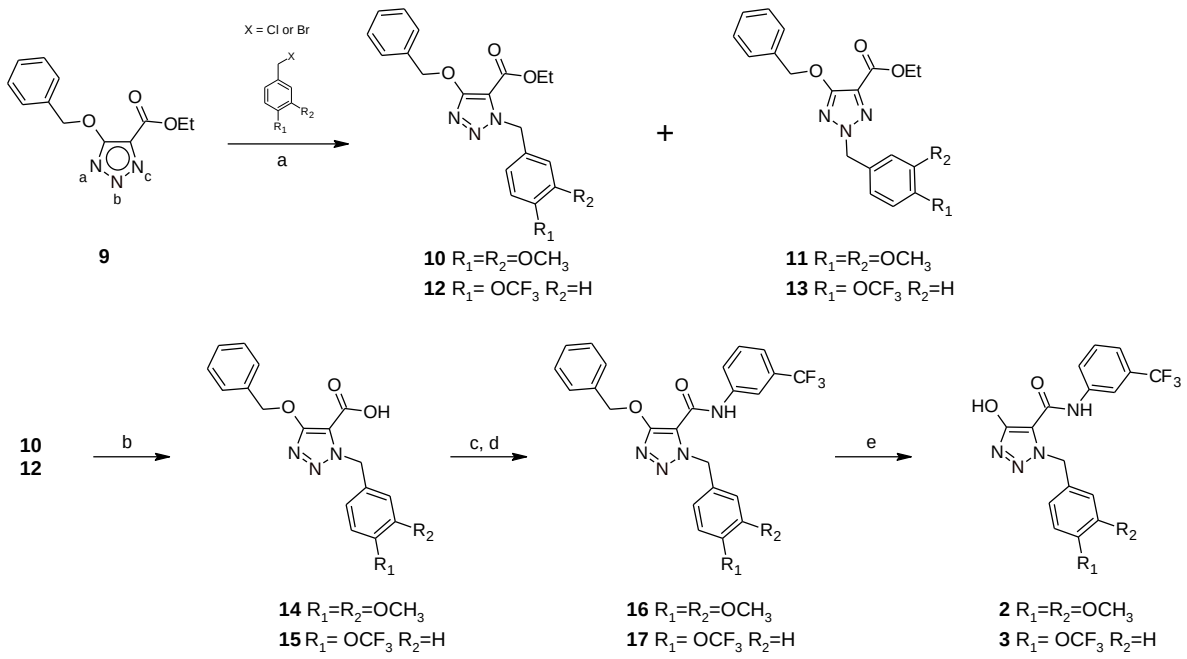

Scheme 1: **a)** Cs_2CO_3, CH_3CN, rt; **b**) 1) NaOH, EtOH, rt; 2) 2M HCl; **c)** $(CO)_2Cl_2$, dry DMF, dry THF, rt; **d)** 3-(trifluoromethyl)aniline, dry pyridine, dry THF, rt; **e)** H_2, Pd/C, dry THF, rt.

The methodology used for the synthesis of the 4-anilino-1,2-benzoxazol-3-ols derivatives **4** and **6 - 8**, described in Scheme 2, follows a described procedure for substituted 1,2-benzoxazol-3-ols.[28] Commercially available 2-bromo-6-fluorobenzoic acid was treated with $(CO)_2Cl_2$ and dry DMF in dry THF to generate acyl chloride **18**, which was coupled with *N*-[(2,4,6-trimethoxyphenyl)methyl]hydroxylamine **19** to afford *N*-hydroxybenzamide **20**. Cyclisation of compound **20** in basic condition yielded the 1,2-benzisoxazol-3-one derivative **21**, where the nitrogen atom of the ring is protected with the 2,4,6-trimethoxybenzyl (Tmob) group. Starting from intermediate **21**, four substituted anilines were used to perform *Buchwald-Hartwig* coupling in which halogenated rings were coupled with aniline derivatives in the presence of a palladium catalyst and a base. Compound **21** was treated with the appropriate aniline, $Pd(OAc)_2$, (±)-2,2-Bis(diphenylphosphino)-1,1-binaphthalene (BINAP) and Cs_2CO_3 in dry toluene at reflux for 5 hours, affording compounds **22 - 25**. After coupling, the target compounds **4** and **6 - 8** were obtained from **22 - 25** by deprotection of Tmob through treatment with trifluoroacetic acid (TFA) and triisopropylsilane in dry DCM.

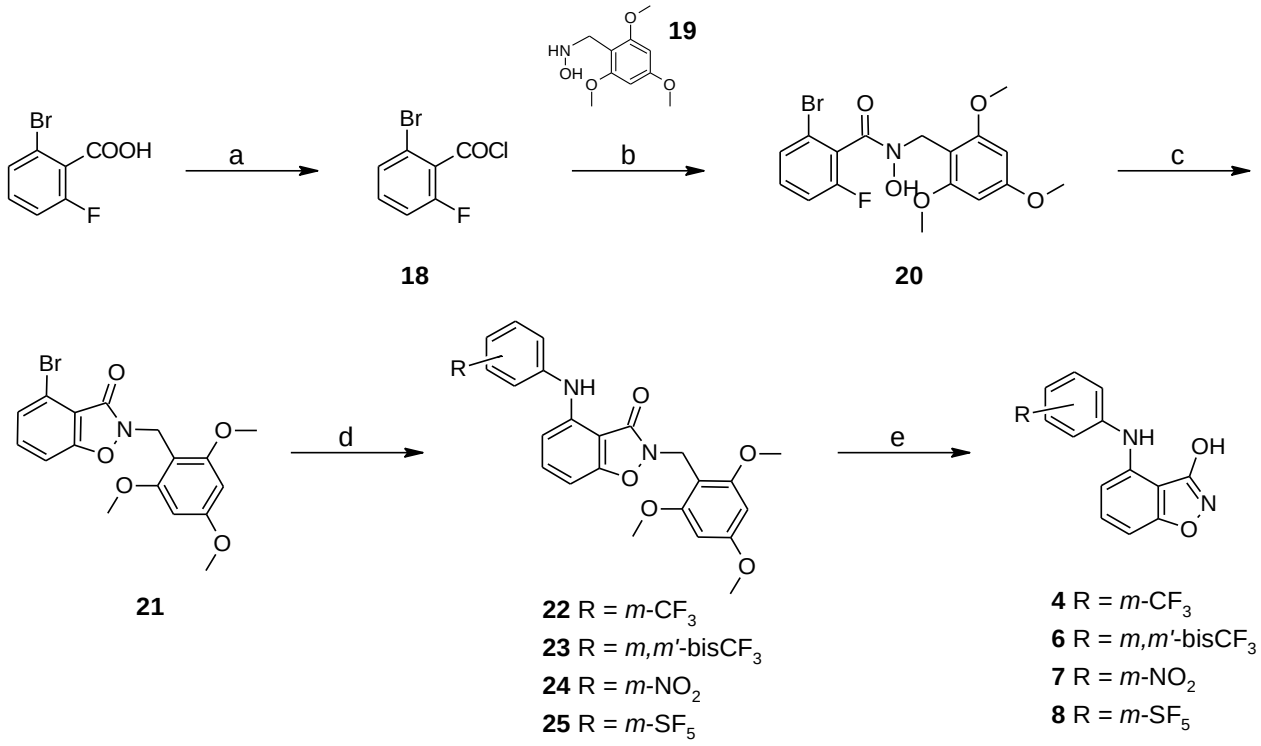

Scheme 2: a) $(CO)_2Cl_2$, dry DMF, dry THF, rt; b) Et_3N, dry THF, rt; c) K_2CO_3, dry DMF, reflux; d) substituted aniline, Cs_2CO_3, BINAP, $Pd(OAc)_2$, dry toluene, reflux; e) TFA, $(i\text{-}Pr)_3SiH$, dry DCM, rt.

Unfortunately, the *Buchwald-Hartwig* coupling conditions failed when applied to affording compound **5** from the appropriate 5-bromo isomer of **21**. This behaviour is probably due to a low reactivity of the bromide group in position 5 of the Tmob protected 1,2-benzisoxazol-3-one. To avoid such problem, a second synthetic route was devised to obtain **5** by changing the sequence order of the reactions (Scheme 3). The *Buchwald-Hartwig* coupling between the 3-trifluoromethylaniline was performed as the first reaction with the methyl 5-bromo-2-fluorobenzoate **26**. Before coupling intermediate **27** with **19**, it was necessary to Boc protect the aniline nitrogen in order to reduce its electron donor properties and thereby activate the *para*-positioned fluorine to nucleophilic substitutions. The treatment of **27** with Boc_2O in dry THF afforded the Boc protected **28**, which was hydrolysed to afford carboxylic acid **29**. This latter was coupled with **19** in the presence of DCC as activating agent to afford **30**. Importantly, when **30** was placed in presence of the basic conditions (K_2CO_3, DMF), it cyclised to afford compound **31**. This result was not observed when the analogue of **30** without Boc protection was treated in the same condition. Finally, the target compound **5** was obtained from **31** by treatment with TFA and triisopropylsilane in order to remove both Boc and Tmob protective groups.

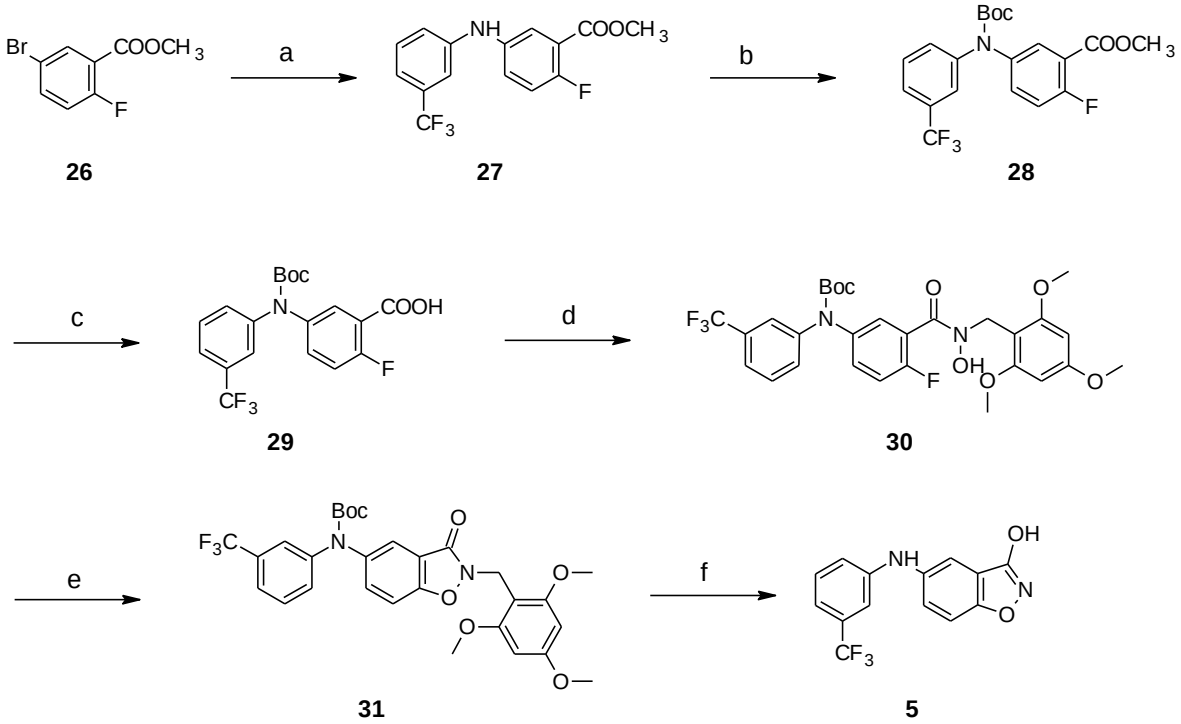

Scheme 3: a) 3-(trifluoromethyl)aniline, Cs_2CO_3, $Pd(OAc)_2$, BINAP, dry toluene, reflux; b) Boc_2O, DMAP, dry THF, rt; c) KOH, EtOH, rt; d) **19**, DCC, DMAP, dry DCM, rt; e) K_2CO_3, dry DMF, reflux; f) TFA, $(i\text{-}Pr)_3SiH$, dry DCM, rt.

2.2 AKR1C3 and AKR1C2 inhibitor screening.

Selective targeting of AKR1C3 over 1C2 is considered critical to effective PCa therapy.[29] Not only does the two isoforms share 86 % sequence similarity, but AKR1C2 is also involved in DHT inactivation and hence its inhibition is undesirable. Accordingly, the inhibitory potencies of compounds **2** - **8** were determined for both AKR1C2 and AKR1C3 and compared with **1** and FLU as controls. To understand their selectivity the ratio of IC_{50} was used as indicator of AKR1C2 and AKR1C3 inhibition (a high ratio shows high selectivity for AKR1C3, Table 1). The inhibitory activity was obtained using recombinant purified enzymes with oxidation of S-tetralol in the presence of $NADP^+$. Although the triazole derivatives **1** - **3** presented IC_{50} values in the similar range as FLU (IC_{50} 0.44 µM), they presented greater than 240-290 fold selectivity for AKR1C3 over AKR1C2. The trifluoromethoxy substituent in the para position of the benzylic moiety appeared to be responsible for increasing activity, as **3** retained potent AKR1C3 inhibition with an IC_{50} value of 0.19 µM and 289-fold selectivity for AKR1C3 over AKR1C2. The inhibitory effect of the 1,2-benzoxazoles series on AKR1C3 and C2 enzymes confirms the hypothesis that the conformational restriction approach to FLU is able to retain potency and improve selectivity of the over the lead compound (Table 1). Noteworthy, both **4** and FLU are equipotent in regard to AKR1C3 inhibition (IC_{50} are 0.55 and 0.44, respectively), but the former is 8-fold more selective in targeting AKR1C3 over AKR1C2. As expected, the shifting of the aniline moiety to position 5 of the 1,2-benzoxazole to mimic the *meta*-FLU's conformation led to reduced potency but greater AKR1C3 selectivity.[20] Indeed, compound **5** displayed an IC_{50} value of 3.48 µM against the AKR1C3 isoform but exhibited 19-fold selectivity for AKR1C3 over AKR1C2 (AKR1C2 IC_{50} = 67 µM). The data support the 3-hydroxy-1,2-benzoxazole as a promising new scaffold for the design of potent and selective AKR1C3 inhibitors.

In attempt to improve the potency and selectivity of compound **4**, modulation of substitution of the aniline moiety was performed. The modulation of FLU derivative by the introduction of a second substituent in the aniline substructure is known[20] to improve potency and

selectivity. Applying a similar strategy, the introduction of a second *m*-trifluoromethyl substituent (compound **6)** doubled the activity and improved drastically the selectivity for AKR1C3 over AKR1C2 enzyme. Specifically, compound **6** displayed an IC_{50} value of 0.26 µM against AKR1C3 and 456-fold selectivity for AKR1C3 over AKR1C2 (IC_{50} 119 µM). This result indicates that the introduction of a second *meta* substituent in the phenyl ring of compound **4** did not have a remarkable effect on the inhibitory potency for AKR1C3, but decreased the affinity for AKR1C2 significantly.

Subsequently, (bio)isosteric replacements of the trifluoromethyl substituent of **4** were performed. Between the possible isostere options, we chose the nitro and pentafluorosulfanyl groups as they retained the activity in the FLU modulations.[20, 30] While the replacement of the *meta*-trifluoromethyl substituent with the nitro group was a successful bioisosteric modulation in the FLU scaffold,[20] when applied to our new 1,2-benzoxazole scaffold (compound **7**) it was detrimental for potency as well as for the selectivity. The IC_{50} values of compound **7** were 1.41 µM and 5.70 µM for AKR1C3 and AKR1C2 respectively, showing that **7** is 2,5-fold less active that its *m*-trifluoromethyl analogue **4** and 1.3-fold less selective. On the contrary, the replacement of the *m*-trifluoromethyl substituent of **4** with the pentafluorosulfanyl (SF_5) moiety (compound **8**) was very successful. The SF_5 group, a bioisoster of the CF_3 and OCF_3 groups, has been gaining greater attention and increased reported usage in the literature.[31] While SF_5-bearing building blocks are typically >5x economically more expensive than the analogous CF_3 compounds, they are particularly attractive to medicinal chemists due to their reported effects on slowing the rates of metabolism.[32] The SF_5 group is a large, very electronegative and lipophilic group. It is also more resistant to acid hydrolysis than either CF_3 or OCF_3.[31] FLU analogues bearing the SF_5 moiety in *meta* and *para* positions have been reported to retain comparable AKR1C3 inhibition activity and selectivity when compared with FLU.[30] Applying this bioisosteric replacement on the 1,2-benzoxazole scaffold, it was evident that the SF_5 derivative **8** gained increase in AKR1C3 potency and selectivity (AKR1C3 vs AKR1C2) to afford a novel analogue that performed similar to compound **4**.

Table 1. Inhibitory effect of compounds **1-8** and FLU against AKR1C3 and AKR1C2 recombinant purified enzymes.

Cpd	Structure	AKR1C3 IC_{50} ± SE (μM)	AKR1C2 IC_{50} ± SE (μM)	Ratio IC_{50} value (1C2:1C3)
FLU	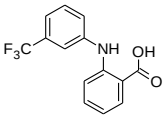	0.44 ± 0.023 [a]	0.53 ± 0.032 [a]	1.2
1	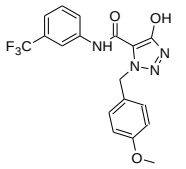	0.31 ± 0.005 [a]	73.23 ± 8.67 [a]	236
2	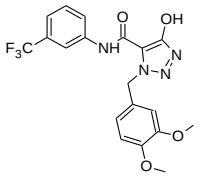	0.40 ± 0.059	108.13 ± 7.42	270
3	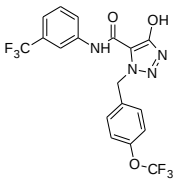	0.19 ± 0.020	54.87 ± 5.01	289
4	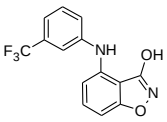	0.55 ± 0.03	4.38 ± 0.49	8
5	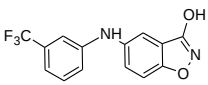	3.48 ± 0.48	66.95 ± 10.67	19
6	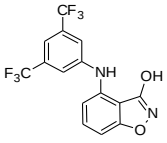	0.26 ± 0.03	118.55 ± 4.86	456
7	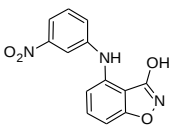	1.41 ± 0.16	5.70 ± 0.30	4

8	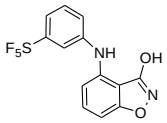	0.31 ± 0.033	4.29 ± 0.144	14

[a] Data from ref.[22]

2.3. COX inhibition.

The compounds were also evaluated against COX1 and COX2 to ensure no off-target effects. Compounds **2 - 8** were assayed for their inhibitor effect on COX1 and COX2 using ovine COX1 (*o*COX1) and human COX2 (*h*COX2). Notably, compounds **2 - 8** did not display significant inhibitory activity on any of the two COX isoforms at the highest concentration evaluated (100 µM) (Table 2)**.**

Table 2. Inhibitory effect of compounds **1**-**8** and FLU against COX1 and COX2.

Compound	*o*COX1 IC_{50} ± SE (µM)	*h*COX2 IC_{50} ± SE (µM)	Ratio IC_{50} value (COX1:AKR1C3)
FLU	14 ± 1[a]	> 100[a] (18 % ± 2) [a, b]	32
1	>100[a] (0)[a, b]	>100[a] (12 % ± 4)[a, b]	> 322
2	> 100 (0)[b]	> 100 (0.87 % ± 0.87)[b]	> 250
3	> 100 (0)[b]	> 100 (0)[b]	> 526
4	> 100 (29 % ± 1)[b]	> 100 (13 % ± 4)[b]	> 182
5	> 100 (29 % ± 3)[b]	> 100 (0)[b]	> 29
6	> 100 (2.1 % ± 2.1)[b]	> 100 (0)[b]	> 385
7	> 100 (0)[b]	> 100 (0.37 % ± 0.37)[b]	> 71
8	> 100 (0)[b]	> 100 (4.3 % ± 2.3)[b]	> 323

[a] Data from ref. [22]
[b] % of inhibition ± SE at 100 µM.

2.4 Inhibition of cell proliferation and PSA expression

The effects of the compounds on cell proliferation were evaluated using the AKR1C3-expressing 22RV1 PCa cell line. Prior to chemosensitivity screening, AKR1C3 protein was confirmed using western blot (Figure 3A). The antiproliferative activity of the compounds was initially performed using the sulforhodamine B (SRB) assay and the IC_{50} values are reported in Figure 3B. All derivatives evaluated, except **7**, exhibited a more pronounced antiproliferative effect than FLU. Triazole **3** (IC_{50} 31.28 µM) and 1,2-benzoxazole **6** (IC_{50} 26.70 µM) were shown to be over 4-fold more potent than FLU (IC_{50} 115 µM, Figure 3B). Since the SRB assay does not distinguish between cytotoxic and cytostatic effects, a colony-growing inhibition investigation was also carried out. In this assay, colonies were observed and counted before and after treatment with selected compounds (triazole derivatives **1** - **3** and 1,2-benzoxazole derivative **6**, Figure 3C-E). 22RV1 cells were incubated for 72 h in the presence of these compounds and the number of viable and dead cells was measured with NucleCounter. The percentage of live cells was significantly reduced in a dose-dependent manner with all tested compounds. Interestingly, when the data for dead cells were analysed (Figure 3D) it was evident that the decrease in cell viability correlated with cell death only for analogues **1** and **6**, while compounds **2** and **3** exhibited a more cytostatic than cytotoxic effect (Figure 3D and 3E).

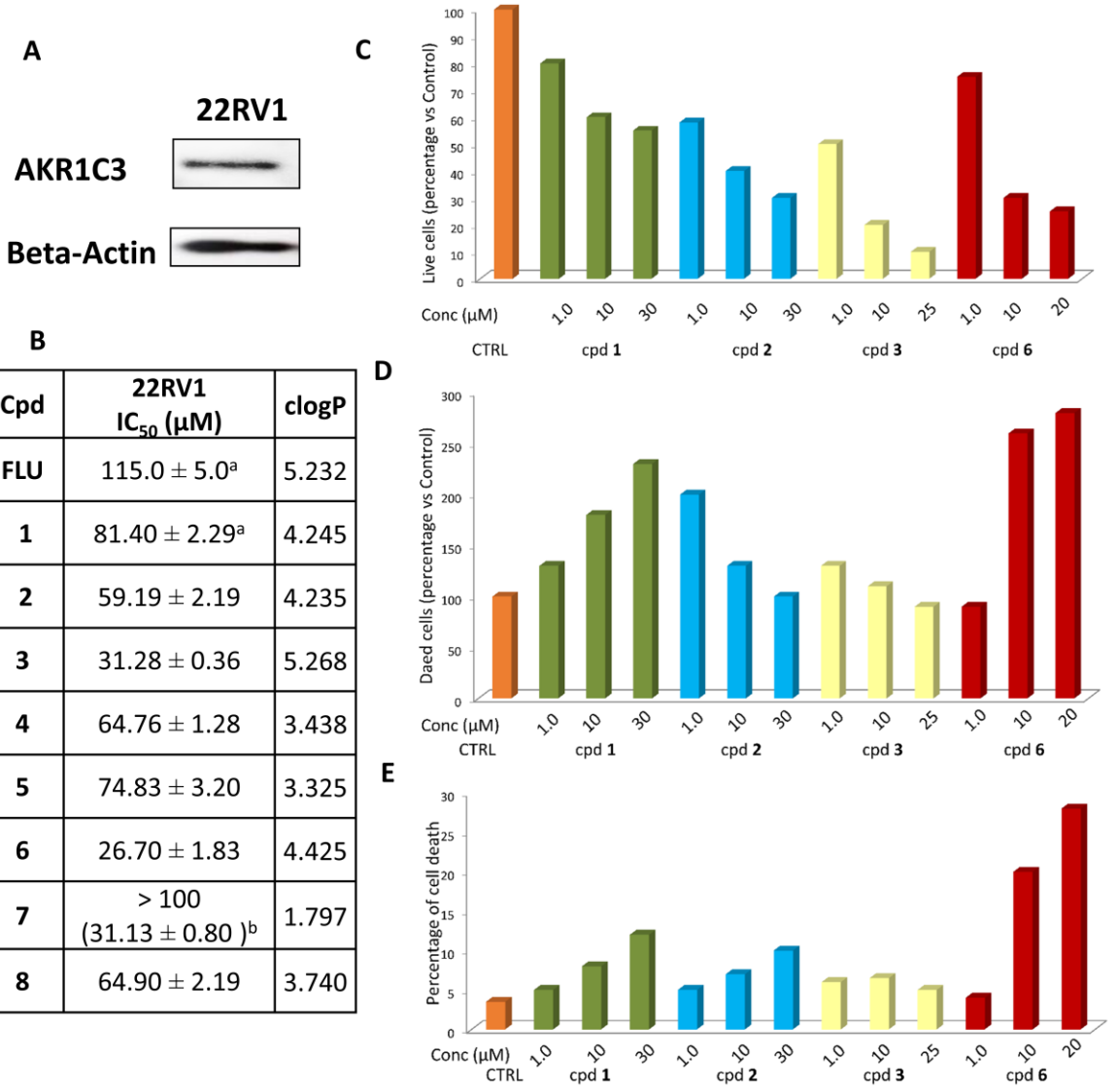

B

Cpd	22RV1 IC_{50} (µM)	clogP
FLU	115.0 ± 5.0[a]	5.232
1	81.40 ± 2.29[a]	4.245
2	59.19 ± 2.19	4.235
3	31.28 ± 0.36	5.268
4	64.76 ± 1.28	3.438
5	74.83 ± 3.20	3.325
6	26.70 ± 1.83	4.425
7	> 100 (31.13 ± 0.80)[b]	1.797
8	64.90 ± 2.19	3.740

Figure 3. Inhibition of cell proliferation. (A) Confirmation of AKR1C3 expression in 22RV1 cells by western blot. (B) IC_{50} values of antiproliferative activity using the SRB assay and cLogP calculated by QikProp.[33] Direct count of live (C) and dead (D) cells by NucleoCounter N100 after incubation for 72 h with compounds, **1**-**3** and **6** at different concentrations. Each column represent the percentage of cells versus control (mean value). Percentage of cell death (mean value) (E). Standard errors were lower than 10%. a) The result is in agreement with our previous study[22]; b) % of inhibition ± SE at 100 µM.

In addition, the effect of the compounds on PSA expression were evaluated using western blot and ELISA assays. Viable cells were lysed from treated 22RV cells described above and western blots were performed. Figure 4A reveal that the PSA expression in the cell extracts was reduced in a dose-dependent manner in cultures treated with compounds **2** and **3**. High doses of **6** also reduced PSA levels in the cell extracts, whereas only very low effects were observed for **1**. However, the differences were much more marked when the secretion of PSA in culture supernatants were measured using ELISA. All compounds resulted in a significant dose-dependent reduction of PSA secretion in treated cells (Figure 4B).

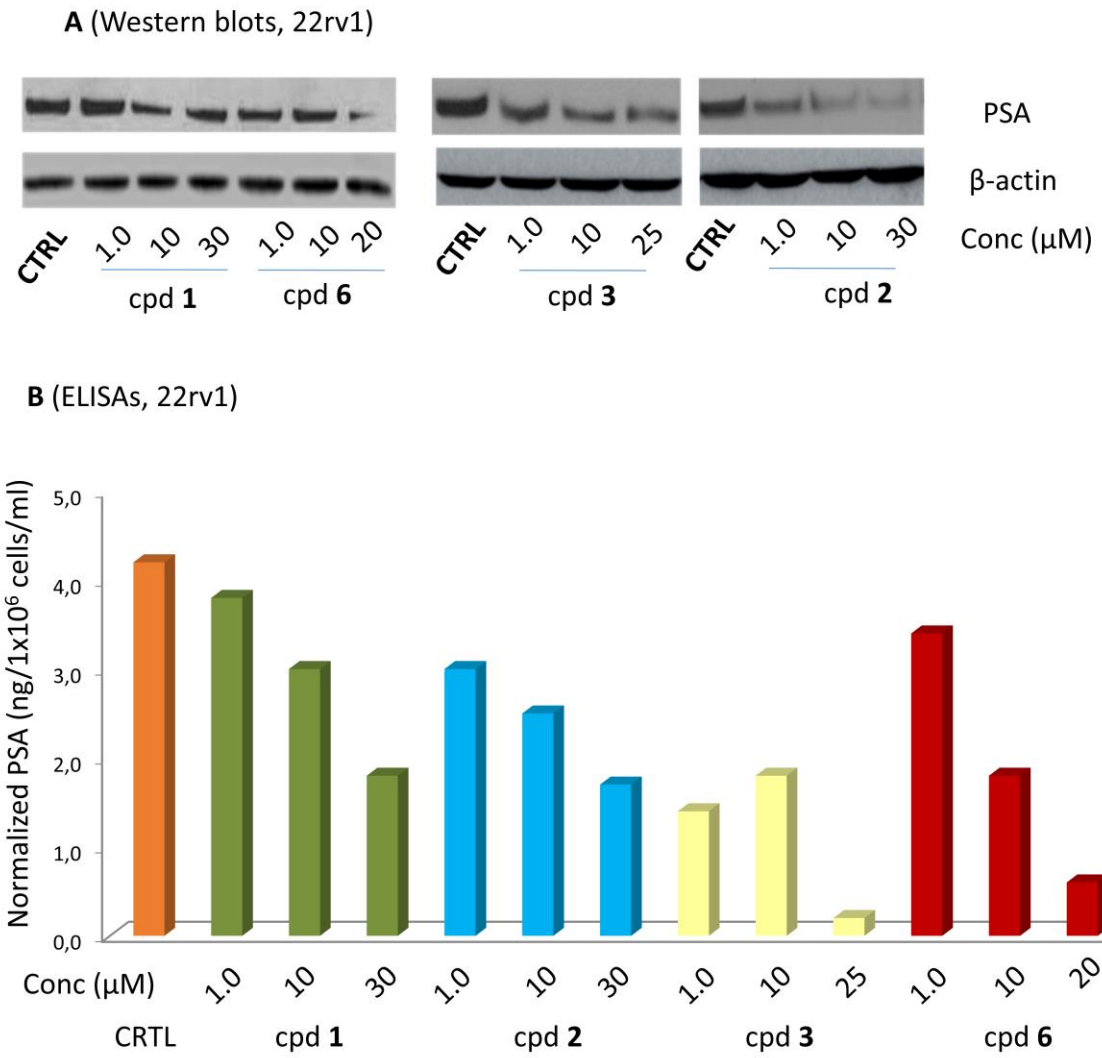

Figure 4. Inhibition of PSA expression. Western blot analysis performed on cell extracts (A) and ELISA assay performed on cell supernatants (secreted PSA) (B) of cultures treated with **1** - **3** and **6** at three different concentrations. Standard errors for ELISA were lower of 10 %.

To explore further the effect of the novel compounds in the steroidogenic pathway, compounds **3** and **6** were investigated for their ability to inhibit testosterone production. After 24 h incubation, androstenedione (AD) was added to each cell with or without compounds **3** and **6** at three concentrations (0.2, 2 and 20 μM). The cell culture media was collected 24 h after treating the cells and both compounds had an effect on the synthesis of testosterone. Compound **3** exerted a dose-dependent effect, whereas **6** had an initial effect at low dose (0.2 μM) but no improved effect at higher doses was observed (Figure 5). Even if compounds **3** and **6** possess similar AKR1C3 inhibitory activity, AKR1C3/1C2 and AKR1C3/COX selectivity ratios, their effects on PSA and testosterone production indicate subtle differences. This result may be related to a number of other key players in the AR dependent and independent pathways of PCa.

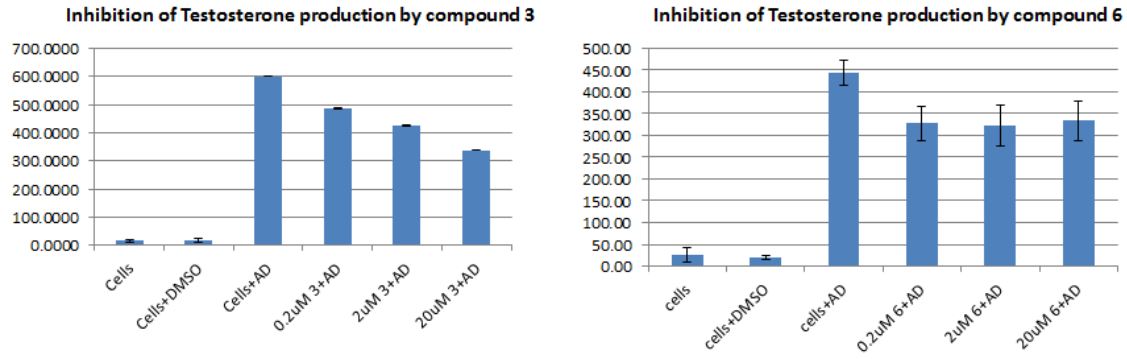

Figure 5. Inhibition of testosterone production. Evaluation of the inhibitory effect of compound **3** and **6** in AD treated 22RV1 cells.

In order to evaluate a possible synergistic effect, compounds **3** and **6** were explored in combination treatments with ABI and ENZA. 22RV1 cells were treated for 72 h with both compounds at 20 µM with or without 10 µM ABI (Figure 6A). The same experiment was carried out by treating cells with or without 20 µM ENZA (Figure 6B). At these concentrations, ABI and ENZA had limited effects on cell growth. When compound **3** or **6** were added together with either ABI or ENZA, the cell viability was reduced by approximately 10-25% compared with either drug alone, indicating a synergistic effect. The 22RV1 cell line was proved to have relative levels of resistance to both ABI and ENZA,[10-12] hence the outcome of the combination experiments are encouraging and indicate the potential of using an AKR1C3 inhibitor to intervene the steroidogenic pathway and effect PSA and testosterone production.

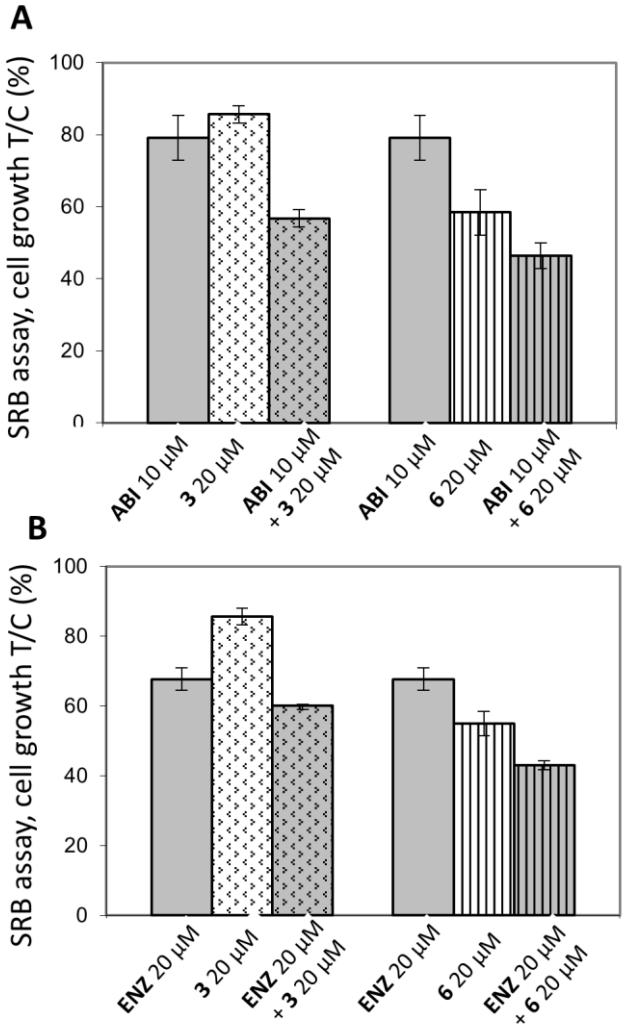

Figure 6. Effect of the co-treatment of compounds **3** and **6** with ABI (A) or ENZA (B) on 22RV1 cell proliferation using the SRB assay. Cells were treated with 20 µM of compounds **3** and **6** with or without 10 µM ABI or 20 µM ENZA for 72 h. Cell growth is expressed as % T/C (mean OD of treated cells/mean OD of control cells X 100).

*2.5 Analysis of the binding mode of compounds **1** and **6** co-crystallised in complex with AKR1C3.*

To support experimental data, co-crystallisation of AKR1C3 in complexes with compound **6** was carried out. Furthermore, we also determined the crystal structures of AKR1C3 in complexes with compound **1**, whose binding mode was speculated by us in previously reported docking studies[22]. The structures were determined by molecular replacement and have been refined to 1.88 Å (**1**, PDB ID: 6F2U) and to 1.30 Å (**6**, PDB ID: 6F78). X-ray data collection and refinement statistics are summarised in Table S16. As reported previously[34], the AKR1C3 ligand-binding pocket is composed by five compartments: an oxyanion site (OS) formed by the cofactor $NADP^+$ and the catalytic residues Tyr55 and His117, a steroid channel (SC) (Tyr24, Leu54, Ser129, Trp227) and three subpockets SP1(Ser118, Asn167, Phe306, Phe311, Tyr319), SP2 (Trp86, Leu122, Ser129, Phe311) and SP3(Tyr24, Glu192, Ser221, Tyr305). Here, the AKR1C3 inhibitors could be clearly identified in the electron density maps in the androstenedione binding site (Figure S17). Compound **6** was found able to establish key interactions inside the OS, involving the hydroxyl group via a double H-bond with Tyr55 and His177, at 2.6 Å and 2.8 Å respectively (Fig. 7). On the other end, the 3,5-

trifluoromethylphenyl moiety binds into the SP1 site, placing one trifluoromethyl towards SP1 and the other close to the Phe311 of SP2.
In regard to the analysis of compound **1**, we found an experimental binding mode that is detached to the one previously docking hypotheses.[22] While the hydroxyl group present in the triazole ring binds into the OS with Tyr55 and His117, producing two H-bond interactions, as predicted by docking, the 4-methoxybenzyl moiety is unexpected found rotated by around 180 degree respect the docking pose, showing a preferred orientation toward SP3 deeply inside the binding pocket. More precisely, this group is located between Phe306 and NADP, making a parallel displacing π-π and T-shape π-π interaction respectively. However, the modulations herein used on benzyl motif in compounds **1**, **2**, **3** affected the activity modestly, that indicates an extended SAR analysis is required to better understand which substitution on 4-methoxybenzyl are beneficial for the activity. Finally, the trifluoromethylphenyl projects into the SP1 pocket, enabling the trifluoromethyl to bind deeply within the cavity. Crystallographic data of AKR1C isoforms show that SP1 pocket in C3 is larger and less discriminating than in C2, this differences should be behind compounds selectivity toward the two isoforms. In order to understand the role of SP1 shape in compound **1** selectivity, a docking study on AKR1C2 was performed. Compound **1** shows a divergent binding mode inside C2 isoform (Figure S18), because the smaller SP1 force the inhibitor to place *m*CF_3-phenyl toward the SC, shifting the molecule that became unable to maintain H-bond interaction inside OS, which is required for AKR1C activity.
The crystallographic data of compounds **1** and **6** well demonstrate the ability of both bioisosteric approaches to effectively mimic carboxylic group into OS. The two co-crystallized compounds demonstrate to have the same contacts as the reference FLU inside SP1 and SP3, moreover compound **1** express a promising additional interaction through the 4-methoxybenzyl moiety that could be a key point to develop more potent and selective AKR1C3 inhibitors.

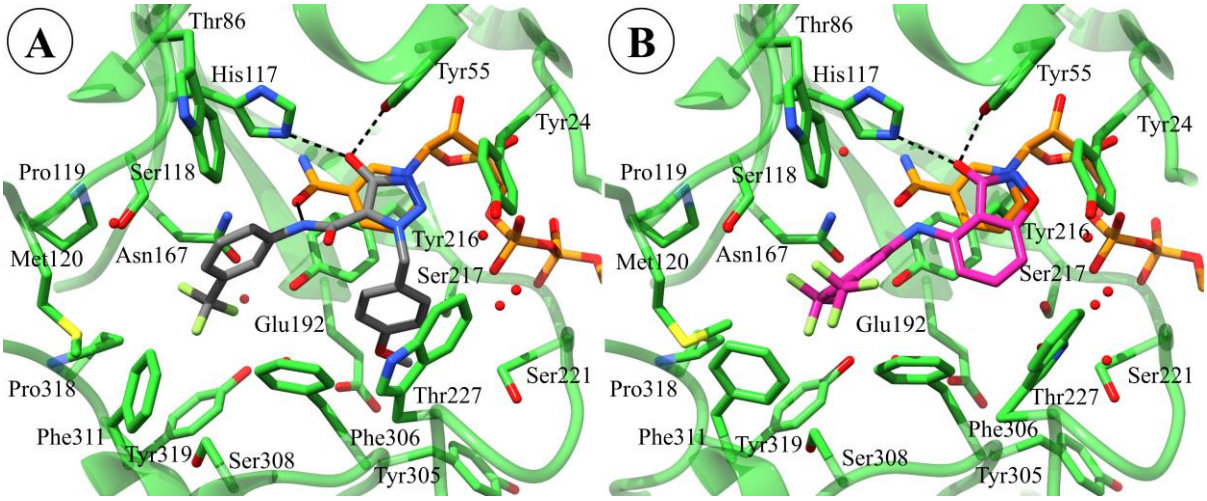

Figure 7. AKR1C3 co-crystallized with compounds **1** in gray (PDB id: 6F2U, A) and **6** in purple (PDB id: 6F78, B). $NADP^+$ is represented in orange. Nitrogen, fluorine, oxygen and sulphur atoms are depicted in blue, green, red and yellow, respectively. Molecular graphics and analyses were performed with the UCSF Chimera package.[35]

3. Conclusions

This study has focused on a new generation of AKR1C3 inhibitors designed by application of a *scaffold hopping* approach to replace the benzoic acid moiety of FLU with hydroxylated azoles. The best compound of the first series, the 4-trifluoromethoxybenzyl substituted analogue **3**, was found to selectively inhibit AKR1C3 activity without any significant AKR1C2 and COX1/2 off-target effects. Although the triazole derivative **3** presented IC_{50} values in the

similar range as FLU, it presented greater than 280-fold selectivity for AKR1C3 over AKR1C2.
The data obtained from the second series support the 3-hydroxy-1,2-benzoxazole as a promising new scaffold for the design of potent and selective AKR1C3 inhibitors. Specifically, compound **6** displayed a submicromolar activity against AKR1C3 and 456-fold selectivity for AKR1C3 over AKR1C2. Compound **3** and **6** were also able to inhibit the cell proliferation of AKR1C3-expressing 22RV1 CRPC cells as well as the PSA expression in a dose-dependent manner. Both compounds showed an effect on the testosterone production, but only compound **3** exerted a dose-dependent effect. These results probably show the complexity in studying the steroidogenic pathway and its multiple parallel outcomes linked to AR dependent and independent pathways. To better clarify this aspect, the effect of **3** and **6** on the AR dependent pathway will be the subject of further investigations. In addition, the inhibition of AKR1C3 activity by compound **3** and **6** were shown to be synergistic in combination with either ENZA and ABI treatment. Taken together, the novel chemical scaffolds here reported provide a promising starting point for the design of more potent AKR1C3 inhibitors with clinical potential use in order to intervene the steroidogenic pathway and reduce both PSA and testosterone production. The crystal structures of the most interesting AKR1C3 inhibitors **1** and **6** will facilitate further optimisation of these lead compounds, aiming to discover new compounds with more drug-like properties and optimal pharmacokinetic characteristics.

4. Experimental section

4.1 Chemistry

4.1.1 General methods

All chemical reagents were obtained from commercial sources (Sigma Aldrich, Alfa Aesar) and used without further purification. Culture media were obtained from Sigma‑Aldrich. Analytical grade solvents (acetonitrile, diisopropyl ether, diethyl ether, dichloromethane [DCM], dimethylformamide [DMF], ethanol 99.8 % v/v, ethyl acetate, methanol [MeOH], petroleum ether b.p. 40 - 60°C [petroleum ether]) were used without further purification. When needed, solvents were dried on 4 Å molecular sieves. Tetrahydrofuran (THF) was distilled immediately prior to use from Na and benzophenone under N_2. Thin layer chromatography (TLC) on silica gel was carried out on 5 x 20 cm plates with 0.25 mm layer thickness to monitor the process of reactions. Anhydrous $MgSO_4$ was used as a drying agent for the organic phases. Purification of compounds was achieved with flash column chromatography on silica gel (Merck Kieselgel 60, 230-400 mesh ASTM) using the eluents indicated or by CombiFlash Rf 200 (Teledyne Isco) with 5–200 mL/min, 200 psi (with automatic injection valve) using RediSep Rf Silica columns (Teledyne Isco) with the eluents indicated. Purity was checked using two analytical methods. HPLC analyses were performed on an UHPLC chromatographic system (Perkin Elmer, Flexar). The analytical column was an UHPLC Acquity CSH Fluoro-Phenyl (2.1x100 mm, 1.7 µm particle size) (Waters). Compounds were dissolved in acetonitrile and injected through a 20 µl loop. The mobile phase consisted of acetonitrile / water with 0.1 % trifluoroacetic acid (ratio between 60 / 40 and 40 / 60, depending on the compound's retention factor). UHPLC analysis were run at flow rates of 0.5 mL/min, and the column effluent was monitored at 215 and 254 nm, referenced against a 360 nm wavelength. Purity of the synthetic intermediates varied between 90 % and 99 % purity. The biological experiments were employed on compounds with a purity of at least 95%. Melting points (m.p.) were measured on a capillary apparatus (Büchi 540) by placing the sample at a temperature 10° C below the m.p. and applying a heating rate of 1° C min^{-1}. All compounds were routinely checked by ^{1}H- and ^{13}C-NMR and mass spectrometry. ^{1}H- and ^{13}C-NMR spectra were performed on a Bruker Avance 300 instrument. For coupling patterns, the following

abbreviations are used: br = broad, s = singlet, d = doublet, dd = doublet of doublets, t = triplet, q = quartet, quint = quintuplet, m = multiplet. Chemical shifts (δ) are given in parts per million (ppm). Accordingly with Zarantonello *et al.*,[36] the ^{13}C NMR spectra of the compounds **8** and **25** are characterized by the presence of the C-SF_5 signals as a quintet of doublets due to the coupling ($^2J_{CF}$ 15 - 18 Hz) with the equatorial four fluorine atoms and with the axial one. The same feature is detected for the carbon atoms in ortho position with respect to the SF_5 group (the $^2J_{CF}$ and the $^3J_{CF}$ coupling constants values with the axial fluorine atom are not reported having a value smaller than 1 Hz). According to Ferraris *et al.*,[28] that reported ^1H spectra of similar *N*-hydroxy-benzamides, ^1H- and ^{13}C-NMR spectra of compounds **20** and **30** showed the presence of the two amide rotamers in the analyzed solutions. ^1H- and ^{13}C-NMR spectra of final compounds **2** – **8** are shown in supplementary. MS spectra were performed on Finnigan-Mat TSQ-700 (70 eV, direct inlet for chemical ionization [CI]) or Waters Micromass ZQ equipped with ESCi source for electrospray ionization mass spectra (ESI). HRMS spectra of final compounds (compounds **2** – **8**) were recorded on LTQ Orbitrap XL plus (Thermo Fisher Scientific, Waltham, MA USA) equipped with an ESI ionization source, with positive or negative ions (Spray capillary voltage: 3000 V (+), 2500 V (-)). Compound **9**[23] was prepared following already described procedure. IR spectra of final compounds (compounds **2** – **8**) were recorded on FT-IR (PerkinElmer SPECTRUM BXII, KBr dispersions) using a diffuse reflectance apparatus DRIFT ACCY (see supplementary to visualize the spectra).

4.1.2. Ethyl 4-(benzyloxy)-1-[(3,4-dimethoxyphenyl)methyl]-1H-1,2,3-triazole-5-carboxylate (**10**) and *ethyl 5-(benzyloxy)-2-[(4-methoxyphenyl)methyl]-2H-1,2,3-triazole-4-carboxylate* (**11**). Cesium carbonate (3.29 g, 10.1 mmol) and 1-(chloromethyl)-3,4-dimethoxybenzene (1.88 g, 10.1 mmol) were added to a solution of **9** (1.00 g, 4.04 mmol) in dry DMF (20 mL). The resulting mixture was stirred at room temperature overnight. When the reaction was complete, the mixture was diluted with water (20 mL) and the pH adjusted to 7 with 0.5 N HCl. The solution was concentrated to half of its volume under reduced pressure, extracted with EtOAc (3 x 30 mL). The combined organic layer was washed with brine, dried over $MgSO_4$ and concentrated under reduced pressure to afford a colorless oil. The latter showed two spots on TLC (eluent: petroleum ether /EtOAc 80/20 v/v) relative to two substituted triazole isomers. The two isomers were separated using flash chromatography (eluent: petroleum ether / EtOAc 80/20 v/v). First eluted isomer, **10**, white solid (m.p. 80.6 – 81.7°C). Yield 31 %. ^1H-NMR (300 MHz, $CDCl_3$): δ 1.34 (3H, *t*, J = 7.1 Hz), 3.83 (3H, *s*), 3.85 (3H, *s*), 4.33 (2H, *q*, J = 7.1 Hz), 5.52 (2H, *s*), 5.75 (2H, *s*), 6.79 (1H, *d*, J = 8.2 Hz), 6.90 – 6.95 (2H, *m*), 7.28 – 7.39 (3H, *m*), 7.46 – 7.49 (2H, *m*); ^{13}C-NMR (75 MHz, $CDCl_3$): δ 14.3, 54.4, 56.0, 61.3, 71.6, 110.7, 111.0, 111.3, 121.0, 127.6, 127.7, 128.2, 128.5, 136.5, 149.1, 149.2, 158.8, 161.3. MS (ESI) 398 $[M + H]^+$.
Second eluted isomer, **11**, white solid (m.p. 95.8 – 97.6°C). Yield 41 %. ^1H-NMR (300 MHz, $CDCl_3$): δ 1.38 (3H, *t*, J = 7.1 Hz), 3.82 (3H, *s*), 3.87 (3H, *s*), 4.40 (2H, *q*, J = 7.1 Hz), 5.33 (2H, *s*), 5.38 (2H, *s*), 6.80 – 6.94 (3H, *m*), 7.29 – 7.38 (3H, *m*), 7.41 – 7.46 (2H, *m*); ^{13}C-NMR (75 MHz, $CDCl_3$): δ 14.5, 56.01, 56.03, 59.6, 61.2, 72.3, 111.1, 111.3, 121.1, 124.1, 126.9, 127.8, 128.2, 128.5, 136.1, 149.2, 149.4, 160.6, 161.0. MS (ESI) 398 $[M + H]^+$.

4.1.3. E*thyl 4-(benzyloxy)-1-(4-methoxybenzyl)-1H-1,2,3-triazole-5-carboxylate* (**12**) and *ethyl 5-(benzyloxy)-2-(4-methoxybenzyl)-2H-1,2,3-triazole-4-carboxylate* (**13**). Cesium carbonate (2.37 g, 7.28 mmol) and 1-(bromomethyl)-4-(trifluoromethoxy)benzene (1.65 g, 6.48 mmol) were added to a solution of **9** (0.90 g, 3.64 mmol) in acetonitrile (20 mL). The resulting mixture was stirred at room temperature overnight. When the reaction was complete, the mixture was diluted with water (20 mL) and the pH adjusted to 7 with 0.5 N HCl. The solution was concentrated to half of its volume under reduced pressure, extracted with EtOAc (3 x 30 mL). The combined organic layer was washed with brine, dried over $MgSO_4$ and concentrated under reduced pressure to afford a colorless oil. The latter showed two spots on TLC (eluent:

petroleum ether /EtOAc 85/15 v/v) relative to two substituted triazole isomers. The two isomers were separated using flash chromatography (eluent: petroleum ether / EtOAc 85/15 v/v). First eluted isomer, **12**, white solid (m.p. 100.0 - 102.1 °C). Yield 33 %. ^{1}H-NMR (300 MHz, $CDCl_3$): δ 1.33 (t, J = 7.1 Hz, 3H), 4.32 (q, J = 7.1 Hz, 2H), 5.53 (s, 2H), 5.81 (s, 2H), 7.16 (d, J = 8.0 Hz, 2H), 7.32 - 7.40 (m, 5H), 7.48 (d, J = 7.2 Hz, 2H). ^{13}C-NMR (75 MHz, $CDCl_3$): δ 14.2, 53.8, 61.5, 71.7, 110.8, 120.5 (q, J = 257.5 Hz), 121.3 (q, J = 0.9 Hz), 127.7, 128.2, 128.6, 129.8, 133.8, 136.4, 149.2 (q, J = 1.8 Hz), 158.7, 161.3. MS (ESI) 422 $[M + H]^+$. Second eluted isomer, **13**, white solid (m.p. 29.3 - 30.5 °C). Yield 45 %. ^{1}H-NMR (300 MHz, $CDCl_3$): δ 1.38 (t, J = 7.1 Hz, 3H), 4.40 (q, J = 7.1 Hz, 2H), 5.34 (s, 2H), 5.44 (s, 2H), 7.17 (d, J = 8.6 Hz, 2H), 7.28 - 7.38 (m, 5H), 7.44 (d, J = 7.9, 2H). ^{13}C-NMR (75 MHz, $CDCl_3$): δ 14.5, 58.8, 61.3, 72.4, 120.5 (q, J = 257.6 Hz), 121.3 (q, J = 0.9 Hz), 124.5, 127.9, 128.3, 128.5, 129.7, 133.1, 136.0, 149.4 (q, J = 1.8 Hz), 160.4, 161.1. MS (ESI) 422 $[M + H]^+$.

4.1.4. 4-(Benzyloxy)-1-[(3,4-dimethoxyphenyl)methyl]-1H-1,2,3-triazole-5-carboxylic acid (**14**). 6M NaOH (0.1 mL) was added to a solution of **10** (0.10 mmol) in ethanol (25 mL) and the reaction mixture was stirred overnight. The resulting solution was neutralized with 2M HCl and concentrated under reduced pressure to half of its volume. 2M HCl was added until pH 1-2, observing precipitation of a white solid. The solid was isolated by filtration and washed with water to give carboxylic acid **14** (m.p. 141.3 – 142.9° C). Yield 92 %. ^{1}H-NMR (300 MHz, DMSO-d_6): δ 3.70 (s, 3H), 3.71 (s, 3H), 5.43 (s, 2H), 5.72 (s, 2H), 6.72 (dd, J = 8.2 Hz and J = 1.2 Hz, 1H), 6.89 - 6.91 (m, 2H), 7.30 - 7.47 (m, 5H), 13.69 (broad s, 1H). ^{13}C-NMR (75 MHz, DMSO-d_6): δ 53.5, 55.4, 55.5, 71.0, 111.0, 111.6, 111.8, 120.0, 127.97, 128.04, 128.1 128.4, 136.5, 148.6, 148.7, 159.2, 160.4. MS (ESI) 370 $[M + H]^+$.

4.1.5. 4-(Benzyloxy)-1-[[4-(trifluoromethoxy)phenyl]methyl]-1H-1,2,3-triazole-5-carboxylic acid (**15**). This product was synthetized following the same procedure of **14,** starting from **12.** White solid (m.p. 179.8 °C - 181.0 °C). Yield 93 %. ^{1}H-NMR (300 MHz, DMSO-d_6): δ 5.44 (s, 2H), 5.84 (s, 2H), 7.28 - 7.48 (m, 9H). ^{13}C-NMR (75 MHz, DMSO-d_6): δ 52.9, 71.2, 111.3, 120.12 (q, J = 256.3 Hz), 121.4 (q, J = 0.9 Hz), 128.1, 128.2, 128.5, 129.5, 135.3, 136.4, 148.0, 159.1, 160.5. MS (ESI) 416 $[M + Na]^+$.

4.1.6. 4-(Benzyloxy)-1-[(3,4-dimethoxyphenyl)methyl]-N-[3-(trifluoromethyl)phenyl]-1H-1,2,3-triazole-5-carboxamide (**16**). Dry DMF (30 µL) and oxalyl chloride (2.40 mmol, 206 µL) were added to a cooled (0°C) solution of **14** (1.00 mmol, 369 mg) in dry THF (20 mL). The reaction was stirred for 3 hours at room temperature under nitrogen atmosphere. The solvent was evaporated under reduced pressure and the residue was dissolved in dry THF (this process was repeated for three times). The resulting acyl chloride was dissolved in dry THF (20 mL) and used without any further purification in the next step. Dry pyridine (242 µL, 3.00 mmol) and 3-trifluoromethylaniline (177 mg, 1.10 mmol) were added to the described solution. The reaction mixture was stirred for 12 hours at room temperature under nitrogen atmosphere. 0.5 M HCl (20 mL) was added to the resulting mixture, which was concentrated under reduced pressure to half of its volume. The resulting suspension was acidified with 0.5 M HCl to pH 2 and extracted with ethyl acetate (3 × 40 mL). The organic phases were collected, washed with brine, dried with Na_2SO_4, and the solvent was evaporated. The crude product was purified using flash chromatography (gradient of petroleum ether /ethyl acetate 80/20 v/v → 0/100 v/v) to obtain the amide **16** as a white solid (150.5 - 151.4 °C). Yield 61%. ^{1}H-NMR (300 MHz, $CDCl_3$): δ 3.84 (s, 3H), 3.86 (s, 3H), 5.60 (s, 2H), 5.89 (s, 2H), 6.81 (d, J = 8.8 Hz, 1H), 7.04 – 7.12 (m, 2H), 7.35 – 7.62 (m, 8H), 7.70 (s, 1H), 8.75 (s, 1H). ^{13}C-NMR (75 MHz, $CDCl_3$): δ 54.4, 55.98, 56.02, 73.4, 111.1, 111.9, 112.4, 116.6 (q, J = 4.2 Hz), 121.3 (q, J = 3.4 Hz), 121.6, 122.9 (q, J = 1.3 Hz), 125.6 (q, J = 250.2 Hz), 127.6, 128.6, 129.1, 129.3, 129.8, 131.4 (q, J = 32.5 Hz), 135.3, 138.0, 149.0, 149.3, 155.6, 158.6. MS (ESI) 513 $[M + H]^+$.

4.1.7. 4-(Benzyloxy)-1-[[4-(trifluoromethoxy)phenyl]methyl]-N-[3-(trifluoromethyl)phenyl]-1H-1,2,3-triazole-5-carboxamide (**17**). This product was synthetized following the same procedure of **16**, starting from **15**. White solid (m.p. 136.5 - 137.1 °C). Yield 69 %. ^{1}H-NMR (300 MHz, $CDCl_3$): δ 5.62 (s, 2H), 5.96 (s, 2H), 7.18 (d, *J* = 8.1 Hz, 2H), 7.31 – 7.66 (m, 11H), 8.75 (s, 1H). ^{13}C-NMR (75 MHz, $CDCl_3$): δ 53.7, 73.5, 112.5, 116.7 (q, *J* = 3.9 Hz), 120.5 (q, *J* = 257.4 Hz), 121.3 (q, *J* = 0.9 Hz), 121.4 (q, *J* = 3.8 Hz), 122.9 (q, *J* = 1.4 Hz), 126.9 (q, *J* = 266.5 Hz) 128.6, 129.1, 129.4, 129.9, 130.3, 131.7 (q, *J* = 32.7 Hz), 133.7, 135.2, 137.8, 149.4 (q, *J* = 1.9 Hz), 155.5, 158.6. MS (ESI) 537 $[M + H]^+$.

4.1.8. 1-[(3,4-Dimethoxyphenyl)methyl]-4-hydroxy-N-[3-(trifluoromethyl)phenyl]-1H-1,2,3-triazole-5-carboxamide (**2**). Compound **16** (0.20 mmol, 102 mg) was dissolved in dry THF (10 mL) and hydrogenated in presence of Pd/C (5% w/w) for 1 hour at atmospheric pressure. The reaction mixture was filtered off through a short layer of celite and the solvent was evaporated under reduced pressure yielding the desired compound. White solid (m.p. 215.1 - 216.8 °C). Yield 90 %. ^{1}H-NMR (300 MHz, DMSO-d_6): δ 3.68 (s, 3H), 3.70 (s, 3H), 5.74 (s, 2H), 6.80 (dd, *J* = 8.3, 1.8 Hz, 1H), 6.87 – 6.99 (m, 2H), 7.47 (d, *J* = 7.8 Hz, 1H), 7.59 (t, *J* = 7.9 Hz, 1H), 7.83 (d, *J* = 8.2 Hz, 1H), 8.16 (s, 1H), 9.98 (s, 1H). ^{13}C-NMR (75 MHz, DMSO-d_6): δ 53.5, 55.3, 55.5, 111.2, 111.7, 111.8, 116.1 (q, *J* = 4.1 Hz), 120.4, 120.5 (q, *J* = 4.6 Hz), 123.7 (q, *J* = 1.1 Hz), 124.1 (q, *J* = 272.4 Hz), 128.0, 129.6 (q, *J* = 31.6 Hz), 130.20, 138.8, 148.6, 148.7, 156.7, 158.5. MS (ESI) 445 $[M + Na]^+$. ESI-HRMS (m/z) $[M + H]^+$ calcd. for $C_{19}H_{17}F_3N_4O_4$ 423.1275, obsd. 423.1271. IR (KBr) ν (cm^{-1}): 2960, 1691, 1640, 1519, 1449, 1340, 1120.

4.1.9. 4-Hydroxy-1-[[4-(trifluoromethoxy)phenyl]methyl]-N-[3-(trifluoromethyl)phenyl]-1H-1,2,3-triazole-5-carboxamide (**3**). This product was synthetized following the same procedure of **2**, starting from **17**. White solid (m.p. 197.8°C - 198.7 °C). Yield 98 %. ^{1}H-NMR (300 MHz, DMSO-d_6): δ 5.87 (s, 2H), 7.35 (d, *J* = 8.3 Hz, 2H), 7.41 (d, *J* = 8.8 Hz, 2H), 7.46 (d, *J* = 7.8 Hz, 1H), 7.58 (t, *J* = 8.0 Hz, 1H), 7.82 (d, *J* = 8.3 Hz, 1H), 8.11 (s, 1H), 9.83 (s, 1H). ^{13}C-NMR (75 MHz, DMSO-d_6): δ 52.8, 11.3, 116.2 (q, *J* = 4.1 Hz), 120.0 (q, *J* = 256.5 Hz), 120.5 (q, *J* = 3.9 Hz), 121.2 (q, *J* = 0.8 Hz), 123.8 (q, *J* = 1.3 Hz), 124.0 (q, *J* = 272.4 Hz), 129.5 (q, *J* = 31.7 Hz), 129.7, 130.0, 135.1, 138.5, 148.0, (q, *J* = 1.8 Hz), 156.4, 158.2. MS (ESI) 447 $[M + H]^+$. ESI-HRMS (m/z) $[M + H]^+$ calcd. for $C_{18}H_{12}F_6N_4O_3$ 447.0886, obsd. 447.0888. IR (KBr) ν (cm^{-1}): 3113, 3036, 1679, 1635, 1575, 1454, 1336, 1278, 1129.

4.1.10. 2-Bromo-6-fluoro-N-hydroxy-N-[(2,4,6-trimethoxyphenyl)methyl]benzamide (**20**). Dry DMF (30 µL) and 2M oxalyl chloride in DCM (18.3 mmol, 9.13 mL) were added to a cooled (0 °C) solution of 2-bromo-6-fluorobenzoic acid (1.60 g, 7.31 mmol) in dry THF (40 mL). The reaction was stirred for 1 hour at room temperature under nitrogen atmosphere, then the solvent was evaporated under reduced pressure and the residue was dissolved in dry THF (this process was repeated for three times). The resulting acyl chloride **18** was dissolved in dry THF (40 mL) and used without any further purification in the next step. Et_3N (3 mL) and N-[(2,4,6-trimethoxyphenyl)methyl]hydroxylamine **19** (1.56 g, 7.31 mmol) were added to the described solution. The reaction mixture was stirred for 2 hours at room temperature under nitrogen atmosphere, then the solvent was evaporated under reduced pressure. The resulting crude material was diluted with DCM, washed with water and brine, dried with Na_2SO_4, and the solvent was evaporated. The crude product was purified through flash chromatography (gradient of petroleum ether /ethyl acetate from 90/10 v/v to 70/30 v/v) to yield the title compound as a yellow solid (m.p. 164.7 - 165.9 °C). Yield 55 %. ^{1}H-NMR (300 MHz, DMSO-d_6): δ 3.65 (s, 3H, major rotamer), 3.75 (s, 6H major and 3H minor rotamers), 3.78 (s, 6H, minor rotamer), 4.30 (d, *J* = 13.7 Hz, 2H minor rotamer), 4.54 (d, *J* = 13.7 Hz, 2H minor rotamer), 4.75 (d, *J* = 13.5 Hz, 2H, major rotamer), 4.87 (d, *J* = 13.5 Hz, 2H, major rotamer),

6.16 (s, 1H minor rotamer), 6.23 (s, 1H, major rotamer), 7.21– 7.57 (m, 3H), 9.47 (s, 1H, major rotamer), 9.62 (s, 1H, minor rotamer). MS (ESI) 414 $[M + H]^+$.

4.1.11. 4-Bromo-2-[(2,4,6-trimethoxyphenyl)methyl]-1,2-benzoxazol-3(2H)-one (**21**). K_2CO_3 (0.805 g, 6.28 mmol) was added to a solution of **20** (1.30 g, 3.14 mmol) in DMF (25 mL) and the mixture was stirred at 120 °C for 30 minutes. The reaction mixture was cooled to room temperature and concentrated under reduced pressure. The resulting solid was partitioned between water (50 mL) and diethyl ether (50 mL), the organic layer was separated and the aqueous layer was extracted with diethyl ether (2 x 50 mL). The combined organic layer was washed with brine, dried over $MgSO_4$ and concentrated under reduced pressure to obtain **21** as a pale yellow solid (m.p. 127.3 - 130.0 °C). Yield 70 %. ^{1}H-NMR (300 MHz, DMSO-d_6): δ 3.74 (s, 6H), 3.78 (s, 3H), 5.04 (s, 2H), 6.25 (s, 2H), 7.39-7.57 (m, 3H). ^{13}C-NMR (75 MHz, DMSO-d_6): δ 38.6, 55.3, 55.9, 90.8, 101.8, 109.8, 114.3, 116.9, 127.4, 134.8, 159.5, 159.8, 160.4, 161.4. MS (ESI) 394 $[M + H]^+$.

4.1.12. General procedure for the preparation of substituted 2-[(2,4,6-trimethoxyphenyl)methyl]-1,2-benzoxazol-3(2H)-ones **22-25***:* the appropriate aniline (1 - 1.4 eq), Cs_2CO_3 (0.179 g, 5.50 mmol), palladium(II) acetate (0.004 g, 0.019 mmol) and BINAP (0.021 g, 0.031mmol) were added to a solution of **21** (0.200 g, 0.507 mmol) in dry toluene under inert atmosphere. The reaction mixture was stirred at 110°C for 3-5 hours, then it was allowed to reach room temperature and the solvent was evaporated. The residue was partitioned between ethyl acetate (30 mL) and HCl 2M (30 mL). The organic layer was separated and the aqueous layer was extracted with ethyl acetate (2 x 30 mL). The combined organic layer was washed with brine, dried over $MgSO_4$ and concentrated under reduced pressure.

4.1.12.1. 4-[3-(Trifluoromethyl)anilino]-2-[(2,4,6-trimethoxyphenyl)methyl]-1,2-benzoxazol-3(2H)-one (**22**). 1 Eq of 3-(trifluoromethyl)aniline was used. The crude product was purified by flash chromatography (petroleum ether/ethyl acetate 80:20 v/v) to give the title compound as a white solid (m.p. 121.3 – 124.5 °C). Yield 73 %. ^{1}H-NMR (300 MHz, DMSO-d_6): δ 3.76 (s, 6H), 3.79 (s, 3H), 5.00 (s, 2H), 6.26 (s, 2H), 6.72 (d, J = 8.2 Hz, 1H), 6.93 (d, J = 8.0 Hz, 1H), 7.34 (d, J = 7.3 Hz, 1H), 7.44 (t, J = 8.1 Hz, 1H), 7.55 (t, J = 7.6 Hz, 1H), 7.68 – 7.59 (m, 2H), 8.62 (s, 1H). ^{13}C-NMR (75 MHz, DMSO-d_6): δ 38.4, 55.3, 55.9, 90.8, 100.3, 102.1, 103.2, 106.3, 116.0, 122.3, 123.0, 126.1 (q, J = 272.7 Hz), 130.1 (q, J = 31.1 Hz), 130.4, 135.2, 141.4, 141.7, 159.6, 160.9, 161.4, 162.6. MS (ESI) 497 $[M + Na]^+$.

4.1.12.2. 4-[3,5-Bis(trifluoromethyl)anilino]-2-[(2,4,6-trimethoxyphenyl)methyl]-1,2-benzoxazol-3(2H)-one (**23**). 1 Eq of 3,5-bis(trifluoromethyl)aniline was used. Flash chromatography eluent: petroleum ether/ethyl acetate 80:20 v/v. Pale yellow solid (m.p. 125.5 - 128.0 °C). Yield 41 %. ^{1}H-NMR (300 MHz, DMSO-d_6): δ 3.76 (s, 6H), 3.78 (s, 3H), 5.01 (s, 2H), 6.21 (s, 2H), 6.77 (d, J = 8.3 Hz, 1H), 6.99 (d, J = 8.0 Hz, 1H), 7.47 (s and t, J = 8.1 Hz, 2H), 7.85 (s, 2H), 8.98 (br s, 1H). ^{13}C-NMR (75 MHz, DMSO-d_6 and $CDCl_3$): δ 39.3, 50.1, 55.6, 90.5, 101.8, 102.0, 104.5, 107.6, 118.1 (q, J = 4.2 Hz), 125.1, 131.4 (q, J = 32.6 Hz), 134.7 (q, J = 0.9 Hz), 141.8 (q, J = 270.0 Hz), 145.2, 149.9, 159.5, 160.8, 161.4, 161.9. MS (ESI) 543 $[M + H]^+$.

4.1.12.3. 4-(3-Nitroanilino)-2-[(2,4,6-trimethoxyphenyl)methyl]-1,2-benzoxazol-3(2H)-one (**24**). 1.4 Eq of 3-nitroaniline was used. The crude material was purified by two subsequent flash chromatography separations (first eluent: petroleum ether/ethyl acetate from 80:20 to 60:40 v/v; second eluent: DCM/ethyl acetate 95:5 v/v). Yellow solid (m.p. 122.2 - 125.0 °C).

Yield 81 %. ^{1}H-NMR (300 MHz, $CDCl_3$): δ 3.83 (s, 3H), 3.84 (s, 6H), 5.18 (s, 2H), 6.15 (s, 2H), 6.58 (d, J = 8.3 Hz, 1H), 6.96 (d, J = 8.1 Hz, 1H), 6.58 (d, J = 8.3 Hz, 1H), 7.60 – 7.42 (m, 2H), 7.87 (d, J = 7.5 Hz, 1H), 8.20 (s, 1H), 8.50 (br s, 1H). ^{13}C-NMR (75 MHz, $CDCl_3$): δ 38.6, 55.5, 56.1, 90.6, 100.6, 103.0, 103.6, 104.9, 113.8, 117.3, 125.8, 130.3, 134.7, 141.7, 142.1, 149.2, 160.1, 161.0, 161.8, 169.1. MS (ESI) 474 $[M + Na]^+$.

4.1.12.4. 4-[3-(Pentafluorosulfanyl)anilino]-2-[(2,4,6-trimethoxyphenyl)methyl]-1,2-benzoxazol-3(2H)-one (**25**). 1.2 Eq of 3-(pentafluorosulfanyl)aniline was used. Flash chromatography eluent: petroleum ether/ethyl acetate 80:20 v/v. Yellow solid (m.p. 123.4-125.2°C). Yield 79 %. ^{1}H-NMR (300 MHz, $CDCl_3$): δ 3.82 (s, 3H), 3.84 (s, 6H), 5.17 (s, 2H), 6.15 (s, 2H), 6.53 (d, J = 8.3 Hz, 1H), 6.86 (d, J = 8.1 Hz, 1H), 7.32 (t, J = 8.2 Hz, 1H), 7.49 – 7.36 (m, 3H), 7.70 (s, 1H), 8.39 (br s, 1H). ^{13}C-NMR (75 MHz, $CDCl_3$): δ 38.6, 55.5, 56.1, 90.6, 100.1, 103.1, 103.3, 104.3, 118.0 (quint, $^{2}J_{CF}$ = 5.0 Hz), 120.3 (quint, $^{3}J_{CF}$ = 4.8 Hz), 123.3, 129.6, 134.7, 140.4 (quint, $^{3}J_{CF}$ = 18.5 Hz) 141.1, 142.3, 160.1, 161.1, 161.8, 163.0. MS (ESI) 533 $[M + H]^+$.

4.1.13. General procedure for the preparation of substituted 1,2-benzoxazol-3-ols **4, 6, 7, 8**: Triisopropylsilane (0.044 g, 0.276 mmol) and TFA (1.5 mL) were added to a solution of the correspondent 2-[(2,4,6-trimethoxyphenyl)methyl]-1,2-benzoxazol-3(2H)-one **(22-25**, 0.256 mmol) in DCM (7.5 mL) and the mixture was stirred for 2 h. The reaction mixture was quenched with water, the organic layer was separated and the aqueous layer was extracted with DCM. The combined organic layer was washed with brine, dried over $MgSO_4$ and concentrated under reduced pressure.

4.1.13.1. 4-[3-(Trifluoromethyl)anilino]-1,2-benzoxazol-3-ol (**4**). White solid (m.p. 148.6 – 149.2 °C, from hexane). Yield 82 %. ^{1}H-NMR (300 MHz, DMSO-d_6): δ 7.06 – 6.84 (t and s, 2H), 7.25 (d, J = 6.4 Hz, 1H), 7.43 (t, J = 8.1 Hz, 1H), 7.61 – 7.48 (m, 3H), 8.30 (s, 1H), 12.55 (br s, 1H). ^{13}C-NMR (75 MHz, DMSO-d_6): δ 102.0, 104.8, 108.1, 114.8 (q, J = 3.2 Hz), 117.4 (q, J = 3.6 Hz), 121.8, 124.2 (q, J = 272.3 Hz), 130.0 (q, J = 31.4 Hz), 130.3, 132.5, 138.7, 143.1, 164.8, 165.4. ESI-HRMS (m/z) $[M + H]^+$ calcd. for $C_{14}H_{10}F_3N_2O_2$ 295.0689, obsd. 295.0685. IR (KBr) ν (cm^{-1}): 3413, 3364, 1656, 1626, 1536, 1333, 1112.

4.1.13.2. 4-[3,5-Bis(trifluoromethyl)anilino]-1,2-benzoxazol-3-ol (**6**). Pale pink solid (m.p. 215.3 - 220.1°C, from hexane). Yield 71 %. ^{1}H-NMR (300 MHz, DMSO-d_6): δ 7.07 (d, J = 7.8 Hz, 1H), 7.15 (d, J = 8.3 Hz, 1H), 7.47 (s, 1H), 7.51 (t, J = 8.1 Hz, 1H), 7.69 (s, 2H), 8.84 (s, 1H), 12.52 (br s, 1H). ^{13}C-NMR (75 MHz, DMSO-d_6): δ 104.1, 106.3, 111.0, 112.48 (q, J = 3.7 Hz), 116.51 (q, J = 2.6 Hz), 123.39 (q, J = 273.0 Hz), 131.10 (q, J = 32.5 Hz), 132.4, 136.7, 145.3, 164.9, 165.0. ESI-HRMS (m/z) $[M + H]^+$ calcd. for $C_{15}H_9F_6N_2O_2$ 363.0563, obsd. 363.0560. IR (KBr) ν (cm^{-1}): 3413, 3373, 1668, 1618, 1531, 1383, 1284, 1123.

4.1.13.3. 4-(3-Nitroanilino)-1,2-benzoxazol-3-ol (**7**). Yellow solid (m.p. 216.1 - 221.0 °C, from acetonitrile). Yield 50 %. ^{1}H-NMR (300 MHz, DMSO-d_6): δ 6.97-7.11 (m, 2H), 7.47 (t, J = 8.3 Hz, 1H), 7.54 (d, J = 8.1 Hz, 1H), 7.62 (d, J = 8.2 Hz, 1H), 7.73 (d, J = 8.0 Hz, 1H), 7.99 – 8.01 (m, 1H), 8.56 (s, 1H), 12.55 (br s, 1H). ^{13}C-NMR (75 MHz, DMSO-d_6): δ 102.9, 105.5, 109.4, 111.7, 115.1, 123.9, 130.4, 138.0, 144.1, 146.8, 148.6, 164.9, 165.2. ESI-HRMS (m/z) $[M + H]^+$ calcd. for $C_{13}H_{10}N_3O_4$ 272.0666, obsd. 272.0664. IR (KBr) ν (cm^{-1}): 3390, 3352, 3094, 1660, 1623, 1534, 1349, 1060.

4.1.13.4. 4-[3-(Pentafluoro-sulfanyl)anilino]-1,2-benzoxazol-3-ol (**8**). White solid (m.p. 174.3 - 177.6°C, from diisopropyl ether). Yield 44 %. ^{1}H-NMR (300 MHz, DMSO-d_6): δ 6.95 (d, J

= 7.8 Hz, 1H), 6.95 (d, *J* = 7.8 Hz, 1H), 7.56 - 7.32 (m, 4H), 7.71 (s, 1H), 8.42 (s, 1H), 12.48 (br s, 1H). ^{13}C-NMR (75 MHz, DMSO-d_6): δ 102.4, 105.1, 108.5, 115.56 (quint, *J* = 5.7 Hz), 117.89 (quint, *J* = 5.3 Hz), 121.4, 130.0, 132.5, 138.4, 143.4, 153.73 (quint, *J* = 14.3 Hz), 164.9, 165.3. ESI-HRMS (m/z) $[M + H]^+$ calcd. for $C_{13}H_{10}F_5N_2O_2S$ 353.0378, obsd. 353.0374. IR (KBr) ν (cm^{-1}): 3413, 3364, 2975, 1664, 1623, 1604, 1528, 1364.

4.1.14. Methyl 2-fluoro-5-[3-(trifluoromethyl)anilino]benzoate (**27**). 3-(Trifluoromethyl)aniline (0.387 g, 2.40 mmol), Cs_2CO_3 (0.912 g, 2.80 mmol), palladium(II) acetate (22.5 mg, 0.100 mmol) and BINAP (0.100 g, 0.160 mmol) were added to a solution of methyl 5-bromo-2-fluorobenzoate **26** (0.466 g, 2.00 mmol) in dry toluene under inert atmosphere. The reaction mixture was stirred at 110 °C overnight, then it was allowed to reach room temperature and the solvent was evaporated. The residue was partitioned between ethyl acetate (100 mL) and 2M HCl (100 mL). The organic layer was separated and the aqueous layer was extracted with ethyl acetate (2 x 100 mL). The combined organic layer was washed with brine, dried over $MgSO_4$ and concentrated under reduced pressure. The crude material was purified through flash chromatography (eluent: petroleum ether / ethyl acetate 90:10 v/v) to yield the title compound **27** as a white solid. M.p. 93.7 – 95.2 °C, from petroleum ether). Yield 71 %. ^{1}H-NMR (300 MHz, DMSO-d_6): δ 3.48 (s, 3H), 7.13 (d, *J* = 7.6 Hz, 1H), 7.33 – 7.18 (m, 3H), 7.50 – 7.34 (m, 2H), 7.45 (t, *J* = 8.0 Hz, 1H), 7.57 (dd, *J* = 6.1, 2.9 Hz, 1H), 8.70 (s, 1H). ^{13}C-NMR (75 MHz, DMSO-d_6): δ 52.4, 111.9 (q, *J* = 4.0 Hz), 115.8 (q, *J* = 4.0 Hz), 118.1 (q, *J* = 23.7 Hz), 118.5 (q, *J* = 11.4 Hz), 119.1, 120.2 (q, *J* = 0.7 Hz), 124.2 (q, *J* = 272.3 Hz), 124.4 (q, *J* = 8.4 Hz), 130.2 (q, *J* = 31.4 Hz), 130.5, 138.6 (q, *J* = 2.7 Hz), 144.3, 155.6 (q, *J* = 251.7 Hz), 164.0 (q, *J* = 3.8 Hz).

4.1.15. Methyl 5-[(tert-butoxycarbonyl)[3-(trifluoromethyl)phenyl]amino]-2-fluorobenzoate (**28**). Di-*tert*-butyl dicarbonate (0.818 g, 3.75 mmol) and 4-dimethylaminopyridine (0.458 g, 3.75 mmol) were added to a solution of **27** (0.783, 2.50 mmol) in dry THF (30 mL). The reaction mixture was stirred at room temperature for 3 hour, then poured in phosphate buffer (pH 5). The resulting solution was extracted twice with diethyl ether and the combined organic layer was washed with brine, dried over $MgSO_4$ and concentrated under reduced pressure. The crude material was purified through flash chromatography (eluent: petroleum ether / ethyl acetate 90:10 v/v) to yield the title compound as a colorless oil. Yield 70%. ^{1}H-NMR (300 MHz, DMSO-d_6): δ 1.38 (s, 9H), 3.84 (s, 3H), 7.43 – 7.33 (m, 1H), 7.54 – 7.44 (m, 1H), 7.66 – 7.53 (m, 3H), 7.72 (s, 1H), 7.77 (dd, *J* = 6.4, 2.8 Hz, 1H). ^{13}C-NMR (75 MHz, DMSO-d_6): δ 27.7, 52.6, 81.5, 117.9 (q, *J* = 23.7 Hz), 118.6 (q, *J* = 11.7 Hz), 122.6 (q, *J* = 3.9 Hz), 123.7 (q, *J* = 3.5 Hz), 123.8 (q, *J* = 272.5 Hz), 129.6 (q, *J* = 31.9 Hz), 130.2, 130.4 (q, *J* = 1.5 Hz), 130.8, 134.3 (q, *J* = 9.7 Hz), 138.3 (q, *J* = 3.5 Hz), 143.0, 152.4, 158.8 (q, *J* = 257.7 Hz), 163.44 (q, *J* = 3.8 Hz). MS (ESI) 436 $[M + Na]^+$.

4.1.16. 5-[(Tert-butoxycarbonyl)[3-(trifluoromethyl)phenyl]amino]-2-fluorobenzoic acid (**29**). 0.2 M KOH (20 mL) was added to a solution of **28** (0.700 g, 1.70 mmol) in EtOH (25 mL), and the reaction mixture was stirred at room temperature overnight. The mixture was concentrated to half of its volume and acidified with 2 M HCl until pH 2 was reached. The suspension was extracted with DCM (3x30 mL) and the combined organic layer was washed with brine, dried over $MgSO_4$ and concentrated under reduced pressure. White solid (m.p. 156.6 - 157.6° C). Yield 81%. ^{1}H-NMR (300 MHz, DMSO-d_6): δ 1.38 (s, 9H), 7.41 – 7.26 (m, 1H), 7.67 – 7.41 (m, 4H), 7.80 – 7.65 (m, 2H). ^{13}C-NMR (75 MHz, DMSO-d_6): δ 27.8, 81.5, 117.8 (q, *J* = 24.6 Hz), 119.8 (q, *J* = 11.6 Hz), 122.6 (q, *J* = 4.3 Hz), 123.7 (q, *J* = 0.7 Hz), 123.9 (q, *J* = 272.5 Hz), 129.6 (q, *J* = 31.9 Hz), 130.2, 130.6 (q, *J* = 1.8 Hz), 130.8, 133.8 (q, *J* = 9.2 Hz), 138.2 (q, *J* = 3.4 Hz), 143.1, 152.5, 159.0 (q, *J* = 256.9 Hz), 164.5 (q, *J* = 3.5 Hz). MS (ESI) 422 $[M + Na]^+$.

4.1.17. 2-Fluoro-N-hydroxy-N-[(2,4,6-trimethoxyphenyl)methyl]-5-[(tert-butoxycarbonyl)[3-(trifluoromethyl)phenyl]amino]benzamide (**30**). *N,N'*-Dicyclohexylcarbodiimide (0.310 g, 1.50 mmol) was added to a solution od 15 (0.600 g, 1.50 mmol) in dry DCM. After 40 minutes, *N*-hydroxy-1-(2,4,6-trimethoxyphenyl)methanamine (0.320, 1.50 mmol) and DMAP (0.018 g, 0.15 mmol) were added and the reaction mixture was stirred at room temperature overnight. The mixture was cooled to 0°C, filtered, and the solid washed with cold DCM. The filtrate was evaporated and the resulting crude purified through flash chromatography (eluent: DCM / ethyl acetate 90:10 v/v) to obtain a white solid (m.p. 169.6 - 171.5° C). Yield 54%. ^{1}H-NMR (300 MHz, DMSO-d_6): δ 1.37 (s, 9H), 3.58 (s, 3H, major rotamer), 3.69 (s, 6H, major and 3H minor rotamer), 3.77 (s, 6H, minor rotamer), 4.48 (s, 2H, minor rotamer), 4.78 (s, 2H, major rotamer), 6.18 - 6.21 (m, 2H), 7.18 – 7.73 (m, 7H), 9.42 (br s, 1H). MS (ESI) 595 $[M + H]^+$.

4.1.18. 2-[(2,4,6-Trimethoxyphenyl)methyl]-5-[(tert-butoxycarbonyl)[3-(trifluoromethyl)phenyl] amino]-1,2-benzoxazol-3(2H)-one (**31**). K_2CO_3 (55.3 mg, 0.400 mmol) was added to a solution of **30** (119 mg, 0.200 mmol) in DMF (7 mL) and the mixture was stirred at 120 °C for 45 minutes. The reaction mixture was cooled to r.t. and concentrated under reduced pressure, the resulting solid was partitioned between water (30 mL) and diethyl ether (30 mL). The organic layer was separated and the aqueous layer was extracted with diethyl ether (2 x 30 mL). The combined organic layer was washed with brine, dried over $MgSO_4$ and concentrated under reduced pressure. The crude product was purified through flash chromatography (eluent: DCM / ethyl acetate 95:5 v/v) to obtain to obtain **31** as a pale yellow solid (m.p. 169.0 – 170.3 °C). Yield 83 %. ^{1}H-NMR (300 MHz, DMSO-d_6): δ 1.37 (s, 9H), 3.73 (s, 6H), 3.77 (s, 3H), 5.05 (s, 2H), 6.20 (s, 2H), 7.35 (d, J = 8.9 Hz, 1H), 7.41 – 7.47 (m, 1H), 7.47 – 7.58 (m, 3H), 7.58 – 7.71 (m, 2H). ^{13}C-NMR (75 MHz, DMSO-d_6): δ 27.7, 48.0, 55.2, 55.7, 81.2, 90.6, 99.0, 101.9, 110.8, 116.6, 121.4 (q, J = 273.4 Hz), 122.9, 123.8, 129.7 (q, J = 32.3 Hz), 129.8, 133.3, 137.7, 138.2, 143.3, 152.6, 157.3, 159.4, 160.6, 161.3. MS (ESI) 575 $[M + H]^+$.

4.1.19. 5-[3-(Trifluoromethyl)anilino]-1,2-benzoxazol-3-ol (**5**). Triisopropylsilane (26 mg, 0.162 mmol) and TFA (1.5 mL) were added to a solution of **31** (87 mg, 0.150 mmol) in DCM (7.5 mL) and the mixture was stirred for 2 h. The reaction mixture was quenched with water, the organic layer was separated and the aqueous layer was extracted twice with DCM. The combined organic layer was washed with brine, dried over Na_2SO_4 and concentrated under reduced pressure. Pale pink solid (m.p. 161.1 – 162.7° C, from hexane). Yield 63 %. ^{1}H-NMR (300 MHz, DMSO-d_6): δ 7.08 (d, J = 7.6 Hz, 1H), 7.20 (s, 1H), 7.26 (d, J = 8.2 Hz, 1H), 7.32 – 7.47 (m, 3H), 7.52 (d, J = 8.9 Hz, 1H), 8.60 (s, 1H), 12.20 (br s, 1H). ^{13}C-NMR (75 MHz, DMSO-d_6): δ 109.4, 111.1 (q, J = 3.9 Hz), 111.2, 115.1 (q, J = 3.8 Hz), 115.1, 118.2, 124.4 (q, J = 272.3 Hz), 124.6, 130.2 (q, J = 31.2 Hz), 130.5, 137.7, 145.5, 159.2, 165.2. MS (ESI) 293 $[M - H]^-$. ESI-HRMS (m/z) $[M + H]^+$ calcd. for $C_{14}H_{10}F_3N_2O_2$ 295.0689, obsd. 295.0686. IR (KBr) ν (cm^{-1}): 3411, 1611, 1561, 1537, 1463, 1341, 1108.

4.2. Expression and purification of recombinant human AKR1C3 and AKR1C2

Escherichia coli BL21 (DE) Codon Plus RP cells expressing recombinant AKR1C3 and AKR1C2 proteins were obtained as previously described.[22] AKR1C3 showed one mutation His5Gln in comparison to the NCBI sequence, described in the literature as a single nucleotide polymorphism very common (refSNP: rs12529). Protein expression and purification were performed as previously described.[22] Briefly, bacteria cells were grown in YT2X media supplemented with ampicillin at 37°C and at OD600 nm = 0.6 the expression was induced by IPTG (0.5 mM) at 24°C for 2 h. Then, bacteria were centrifuge and lysed with four freeze-thaw cycles in presence of lysozyme and protease inhibitors. DNA was digested with benzonase (25

U) in presence of $MgCl_2$ 5 mM. The lysate was centrifuged for 30 min at 13,000 x g and the supernatant was collected. AKR1C3 and AKR1C2 were affinity purified via N-terminal GST-tag on glutathione (GT) sepharose (GE-Healthcare) and cleaved of by thrombin according to the manufacturer's protocol. Expression and purification was monitored by SDS-PAGE.

4.3 In vitro AKR1C3 and AKR1C2 inhibition assays

The inhibition assays were performed on purified recombinant enzymes as previously described.[22] Briefly, the enzymatic reaction was fluorimetrically (exc/em; 340 nm/ 460 nm) monitored by the measurement of NADPH production on a "Ensight" plate reader (Perkin Elmer) at 37°C. Assay mixture contained S-tetralol (in ETOH), inhibitor (in ETOH), 100 mM phosphate buffer, pH 7, 200 µM $NADP^+$, and purified recombinant enzyme (30 µl) in a final volume of 200 µl and 10 % ETOH were added in 96-well plate. The S-tetralol concentration used in the AKR1C2 and AKR1C3 inhibition assay were 15 µM and 160 µM, respectively, the same as the Km described for the respective isoforms under the same experimental conditions. Percent inhibition with respect to the controls containing the same amount of solvent, without inhibitor, was calculated from the initial velocities, obtained by linear regression of the progress curve, at different concentrations of inhibitor. The IC_{50} values were obtained using PRISM 7.0, GraphPad Software. The values are the means of two separate experiments each carried out in triplicate.

4.4 COX1 and COX2 inhibition assays

References and selected compounds were tested for their ability to inhibit COX1 and COX2 using a COX (ovine/human) Inhibitor Screening Assay Kit (Cayman Chemical Co., Ann Arbor, MI), following manufacturer's instructions. The assay directly measured $PGF_{2\alpha}$ by $SnCl_2$ reduction of COX-derived PGH_2 produced in the COX reaction. The prostanoid product was quantified *via* enzyme immunosorbent assay (ELISA); absorbance measurements were obtained on a PerkinElmer 2030 Multilabel Reader. IC_{50} values were obtained by linear regression using PRISM 7.0, GraphPad Software. Results were calculated as mean value ± standard error (SE) of at least three experiments.

4.5 Tumor cell lines and cell culture

22RV1 castration-resistant prostate cancer cells were used. Cells were routinely maintained as monolayers in RPMI supplemented with 10 % (v/v) fetal calf serum, 2 % (v/v) penicillin-streptomycin and 0.03% L-glutamine. Cells were grown at 37°C in a humidified atmosphere containing 5 % CO_2.

4.6 Cell proliferation assay

Cell growth inhibition was evaluated by sulforhodamine B colorimetric proliferation assay (SRB assay) modified by Vichai and Kirtikara, as previously described.[37, 38] 10.000 cells/well were seeded into 96-well plates in RPMI containing 10% charcoal stripped serum, and incubated for 24 hours. Then, various dilutions of inhibitors in ethanol were added in triplicate, and incubated for 72 h. Control cells were incubated with the same final concentration of ethanol (maximum concentration 1 % v/v). For co-treatment experiments, 22RV1 cells were treated with ABI (10 µM) or ENZA (20 µM) with or without compounds 3 and 6 (20 µM) for 72 h.
The statistical analysis were performed with PRISM 7.0, GraphPad Software. The values are the means of two separate experiments each carried out in triplicate.

4.7. Viability/death cell determination

22RV1 cell lines cultured as above were trypsinized at 72 h and counted by using the NucleoCounter® NC-200™ (ChemoMetech, Allerod, Denmark) and the propidium iodine uptake to distinguish dead (uptake of propidium iodine without lysis of cells) and total cells (after lysis). The difference between total and dead cells is the number of live cells.[39]

4.8 Western blot

Protein extraction from both untreated and treated 22RV1 cells was conducted using a RIPA lysis buffer containing the Complete Protease Inhibitor Cocktail (Roche Molecular Biochemicals). The protein concentration was determined by use of a Bradford assay. Protein samples (20 µg) were denatured by Tris-Glycine SDS Sample Buffer (Biorad), aliquots of which were loaded into polyacrylamide gel wells alongside identical volumes of β-actin. Polyacrylamide gel electrophoresis (SDS-PAGE) was run at 120V for 2 hours. Proteins were transferred to nitrocellulose membrane (GE Healthcare Life Sciences) by electro-blotting at 300 mA for 3 hours, then blocked using 5% dried milk powder in 0.05% Tris-buffered saline (TBS) + Tween 20. The membrane was incubated overnight at 4°C on a shaker with specific primary antibody diluted in 5% milk powder 0.05% TBS + Tween 20. The following primary antibodies were used: mouse β-actin (1: 20:000, Sigma-Aldrich), mouse monoclonal anti-AKR1C3 (1:333, Sigma Aldrich), goat polyclonal PSA (C-19) (1:500, sc-7638 Santa Cruz Biotechnology). The membrane was washed with TBS and incubated with a HRP-conjugated secondary antibody (Santa-Cruz Biotechnology) diluted 1:5000 in 5% dried milk powder with 0.05% TBS + Tween 20 at room temperature. Ponceau Red Staining (Sigma-Aldrich) was used to ensure samples were equally loaded in SDS-PAGE. Visualisation was achieved using a chemiluminescent substrate (Amersham ECL, GE Healthcare Life Sciences) and captured into Kodak film.

4.9 Determination of PSA expression by Elisa

22RV1 cell lines are cultured as above described. Supernatants were collected, centrifuged to eliminate cell debris and stored at -80 °C until to use when 100 µl were analyzed by a PSA (Total) Human ELISA Kit (Termofisher scientific (Life Technologies Italia, Monza Italy). PSA (ng/ml) were normalized for the cell number. The statistical analysis were performed with PRISM 7.0, GraphPad Software. Results are representative of one replicated experiment performed in triplicate.

4.10 Inhibition of AKR1C3-Mediated production of testosterone in 22RV1 cells

22RV1 cells were seeded into 96-well plates in RPMI media containing 10% charcoal stripped serum, at a density of 30,000 cells per well, and were incubated at 37 °C with 5% CO_2 for 24 h. Compound 3 and Compound 6 were added to the wells at 4 different concentrations and incubated for 1 h. Equimolar (28 nM) concentration of androstenedione was then added to the wells. The plate was returned to the incubator for a further 24 h. Cell supernatant was removed for analysis of testosterone by ELISA following the manufacturer's guide (Testosterone ELISA kit was purchased from Cayman Chemical Company). The statistical analysis were performed with PRISM 7.0, GraphPad Software. The values are the means of two separate experiments each carried out in triplicate.

4.10 Protein expression, purification and crystallization

Plasmid coding for human AKR1C3[22] was modified by removing the thrombin cleavage-site and adding the TEV (Tobacco Etch Virus) cleavage-site. The new plasmid construct was transformed into *E. coli* BL21 (DE) Codon Plus RP (Agilent Technologies).
The cells were grown in LB media supplemented with ampicillin (100 µg/mL) and chloramphenicol (34 µg/mL) at 37 °C with continuous shaking at 200 rpm. At OD600nm = 0.5 the expression was induced by IPTG (0.4 mM) and the temperature was lower to 22 °C for overnight. The cell pellet was resuspended in the binding buffer A (10 mM Na_2HPO_4, 1.8 mM KH_2PO_4, 140 mM NaCl, 2.7 mM KCl pH 7.3) supplemented with DNase 1 (0.1 µg per gram of wet cells), lysozyme (0.1 mg/ml). The suspension was passed through the emulsiflex 3 times at 12000 psi at 4 °C. The cell lysate was centrifuged at 40000 x g, 4 °C, 1 hour in JA25 rotor. The clarified lysate was loaded on to 5 ml GST TRAP column (GE healthcare) prequlibriated with the binding buffer. The loaded column was washed until no more protein was eluted. The protein was eluted using the elution buffer 50 mM Tris-HCl pH 8.0, 10 mM Glutathione reduced. The eluted fractions were pooled and subjected to overnight TEV protease digestion at 4 °C to remove GST tag. TEV protease was used in 1:100 dilution for the digestion. Next day, protein solution was loaded on to a 5 ml His TRAP column equilibriated with buffer Tris-HCl pH 8.0, NaCl 150 mM, DTT 1mM. The flowthrough containing cleaved AKR1C3 protein was collected and concentrated using Vivaspin 10 kDa cutoff. For final polishing step, size exclusion chromatography was performed using superdex 200 column (GE healthcare). The concentrated protein was applied to s 200 column with 10 mM potassium phosphate pH 7, 1 mM EDTA and 1 mM DTT. Fractions were run on the SDS PAGE to check the purity. Pure fractions containing AKR1C3 were pooled and concentrated to 75 mg/ml.

Co-crystals of AKR1C3 and inhibitors were obtained using hanging vapour diffusion method. Both NADP and inhibitor were added in final concentration of 2 mM to the protein solution (25 mg/ml) and incubated overnight at 4 °C. For crystallization, 3 µl the overnight incubated protein was mixed with the reservoir solution (100 mM MES pH 6.0, 12-25% PEG 8000).[40] The crystallization plates were incubated both, at 4 °C and 20 °C. Crystals for both the inhibitors appeared in 100 mM MES pH 6.0, 25% PEG 8000. Crystals for compound 1 appeared at 20 °C while that of 6 formed at 4 °C. The crystals were cryoprotected using 20% ethylene glycol in mother liquor prior to cryo-cooling.

4.11 X-ray data collection, structure determination and refinement

X-ray diffraction data of compound 6 was collected at ID23-1 while for compound 1 was collected at ID30A-3 beamlines of ESRF. X-ray diffraction spots were processed using XDS, pointless and Scala.[41] PDB id1ry09[40] was used as the molecular replacement template for the structure determination using Phaser of PHENIX suite.[42] Both structures were refined using PHENIX. Data collection and refinement statistics are summarised in Table S16.

4.12 Docking

The structures of compounds **1** were built in their dissociated forms using the 2D Sketcher tool implemented in Maestro GUI. Ligand docking was performed using Schrödinger GLIDE extra precision (XP) protocol.[43] or this purpose, the X-ray crystallographic structure of AKR1C2 was retrieved from RCSB Database (PDB code: 4JQA). Before docking, the crystal structure of the protein underwent an optimization process using the Protein Preparation Wizard tool, implemented in Maestro™ GUI. Missing hydrogen atoms were added and bond orders were assigned. Then, DMS, non-structural water molecules and impurities (such as solvent molecules) were removed. Reorienting automatically optimized the hydrogen bond network: hydroxyl and thiol groups, amide groups of asparagine (Asn) and glutamine (Gln), and the imidazole ring in histidine (His). Moreover, the protonation states prediction of His—aspartic

acid (Asp), glutamic acid (Glu), and tautomeric states of His—were accomplished using PROPKA.™ A grid of 10 Å x 10 Å x 10 Å (*x, y,* and *z*) was created and centred on the co-crystalized ligand mefenamic acid.

AUTHOR INFORMATION

Corresponding Authors: *
Phone: +39-0116707180. Fax: +39-0116707162, *e*-mail: marco.lolli@unito.it.
Phone: +39-0116706864 . *e*-mail: simona.oliaro@unito.it.
Notes. The authors declare no competing financial interest.

ABBREVIATIONS USED

Aldo-keto reductase 1C3 isoform (AKR1C3), Prostate cancer (PCa), androgen deprivation therapy (ADT), castration-resistant prostate cancer (CRPC), androgen receptor (AR), flufenamic acid (FLU), sub-pocket 2 (SP2), sub-pocket 1 (SP1), cyclooxygenase (COX), aldo-keto reductase 1C2 isoform (AKR1C2), dichloromethane (DCM), dimethylformamide (DMF), methanol (MeOH), Quantum mechanics/molecular mechanics (QM/MM), QM-Polarized Ligand Docking (QPLD), hexadeuterodimethyl sulfoxide (DMSO-d_6), deuterochloroform ($CDCl_3$), tetradeuteromethanol (CD_3OD), deuterated acetone $(CD_3)_2CO$), PSA (prostatic serum antigen).

ACKNOWLEDGEMENTS

We thank Prof Norman J. Maitland (University of York) for provision of the 22RV1 PC cell line. This research was financially supported by the University of Turin (*Ricerca Locale grant* 2015-2017) and Prostate Cancer UK grant S12-027.

Appendix A. Supplementary data

Supplementary data related to this article can be found at: XXXXXX

References

[1] T.M. Penning, M.E. Burczynski, J.M. Jez, C.F. Hung, H.K. Lin, H. Ma, M. Moore, N. Palackal, K. Ratnam, Human 3alpha-hydroxysteroid dehydrogenase isoforms (AKR1C1-AKR1C4) of the aldo-keto reductase superfamily: functional plasticity and tissue distribution reveals roles in the inactivation and formation of male and female sex hormones, Biochem J, 351 (2000) 67-77.
[2] A. Egan, Y. Dong, H. Zhang, Y. Qi, S.P. Balk, O. Sartor, Castration-resistant prostate cancer: Adaptive responses in the androgen axis, Cancer Treatment Reviews, 40 (2014) 426-433.
[3] A.C. Pippione, D. Boschi, K. Pors, S. Oliaro-Bosso, M.L. Lolli, Androgen-AR axis in primary and metastatic prostate cancer: chasing steroidogenic enzymes for therapeutic intervention, Journal of Cancer Metastasis and Treatment, 3 (2017) 328-361.
[4] T. Seisen, M. Roupret, F. Gomez, G.G. Malouf, S.F. Shariat, B. Peyronnet, J.P. Spano, G. Cancel-Tassin, O. Cussenot, A comprehensive review of genomic landscape, biomarkers and treatment sequencing in castration-resistant prostate cancer, Cancer Treat Rev, 48 (2016) 25-33.
[5] J. Kumagai, J. Hofland, S. Erkens-Schulze, N.F. Dits, J. Steenbergen, G. Jenster, Y. Homma, F.H. de Jong, W.M. van Weerden, Intratumoral conversion of adrenal androgen

precursors drives androgen receptor-activated cell growth in prostate cancer more potently than de novo steroidogenesis, The Prostate, 73 (2013) 1636-1650.
[6] T.M. Penning, Mechanisms of drug resistance that target the androgen axis in castration resistant prostate cancer (CRPC), J Steroid Biochem Mol Biol, 153 (2015) 105-113.
[7] M. Sakai, D.B. Martinez-Arguelles, A.G. Aprikian, A.M. Magliocco, V. Papadopoulos, De novo steroid biosynthesis in human prostate cell lines and biopsies, The Prostate, 76 (2016) 575-587.
[8] S.Q. Sun, X. Gu, X.S. Gao, Y. Li, H. Yu, W. Xiong, H. Yu, W. Wang, Y. Li, Y. Teng, D. Zhou, Overexpression of AKR1C3 significantly enhances human prostate cancer cells resistance to radiation, Oncotarget, 7 (2016) 48050-48058.
[9] C. Liu, C.M. Armstrong, W. Lou, A. Lombard, C.P. Evans, A.C. Gao, Inhibition of AKR1C3 activation overcomes resistance to abiraterone in advanced prostate cancer, Mol Cancer Ther, 16 (2017) 35-44.
[10] C. Liu, W. Lou, Y. Zhu, J.C. Yang, N. Nadiminty, N.W. Gaikwad, C.P. Evans, A.C. Gao, Intracrine androgens and AKR1C3 activation confer resistance to enzalutamide in prostate cancer, Cancer Res, 75 (2015) 1413-1422.
[11] Y.D. Yin, M. Fu, D.G. Brooke, D.M. Heinrich, W.A. Denny, S.M. Jamieson, The Activity of SN33638, an Inhibitor of AKR1C3, on testosterone and 17beta-estradiol production and function in castration-resistant prostate cancer and ER-positive breast cancer, Front Oncol, 4 (2014) 159.
[12] W. Zhou, P. Limonta, AKR1C3 inhibition therapy in castration-resistant prostate cancer and breast cancer: lessons from responses to SN33638, Front Oncol, 4 (2014) 162.
[13] Y. Loriot, K. Fizazi, R.J. Jones, J. Van den Brande, R.L. Molife, A. Omlin, N.D. James, E. Baskin-Bey, M. Heeringa, B. Baron, G.M. Holtkamp, T. Ouatas, J.S. De Bono, Safety, tolerability and anti-tumour activity of the androgen biosynthesis inhibitor ASP9521 in patients with metastatic castration-resistant prostate cancer: multi-centre phase I/II study, Invest New Drugs, 32 (2014) 995-1004.
[14] A. Adeniji, M.J. Uddin, T. Zang, D. Tamae, P. Wangtrakuldee, L.J. Marnett, T.M. Penning, Discovery of (R)-2-(6-Methoxynaphthalen-2-yl)butanoic Acid as a Potent and Selective Aldo-keto Reductase 1C3 Inhibitor, J Med Chem, 59 (2016) 7431-7444.
[15] T. Zang, K. Verma, M. Chen, Y. Jin, P.C. Trippier, T.M. Penning, Screening baccharin analogs as selective inhibitors against type 5 17β-hydroxysteroid dehydrogenase (AKR1C3), Chem.-Biol. Interact., 234 (2015) 339-348.
[16] J.U. Flanagan, G.J. Atwell, D.M. Heinrich, D.G. Brooke, S. Silva, L.J. Rigoreau, E. Trivier, A.P. Turnbull, T. Raynham, S.M. Jamieson, W.A. Denny, Morpholylureas are a new class of potent and selective inhibitors of the type 5 17-beta-hydroxysteroid dehydrogenase (AKR1C3), Bioorg Med Chem, 22 (2014) 967-977.
[17] A.J. Liedtke, A.O. Adeniji, M. Chen, M.C. Byrns, Y. Jin, D.W. Christianson, L.J. Marnett, T.M. Penning, Development of Potent and Selective Indomethacin Analogues for the Inhibition of AKR1C3 (Type 5 17β-Hydroxysteroid Dehydrogenase/Prostaglandin F Synthase) in Castrate-Resistant Prostate Cancer, J Med Chem, 56 (2013) 2429-2446.
[18] T.M. Penning, Aldo-Keto Reductase (AKR) 1C3 inhibitors: a patent review, Expert Opin Ther Pat, 27 (2017) 1329-1340.
[19] T.M. Penning, P. Talalay, Inhibition of a major NAD(P)-linked oxidoreductase from rat liver cytosol by steroidal and nonsteroidal anti-inflammatory agents and by prostaglandins, Proc Natl Acad Sci U S A, 80 (1983) 4504-4508.
[20] A.O. Adeniji, B.M. Twenter, M.C. Byrns, Y. Jin, M. Chen, J.D. Winkler, T.M. Penning, Development of Potent and Selective Inhibitors of Aldo-Keto Reductase 1C3 (Type 5 17β-Hydroxysteroid Dehydrogenase) Based on N-Phenyl-Aminobenzoates and Their Structure-Activity Relationships, J. Med. Chem., 55 (2012) 2311-2323.

[21] R. Pouplana, C. Perez, J. Sanchez, J.J. Lozano, P. Puig-Parellada, The structural and electronical factors that contribute affinity for the time-dependent inhibition of PGHS-1 by indomethacin, diclofenac and fenamates, J Comput Aid Mol Des, 13 (1999) 297-313.
[22] A.C. Pippione, A. Giraudo, D. Bonanni, I.M. Carnovale, E. Marini, C. Cena, A. Costale, D. Zonari, K. Pors, M. Sadiq, D. Boschi, S. Oliaro-Bosso, M.L. Lolli, Hydroxytriazole derivatives as potent and selective aldo-keto reductase 1C3 (AKR1C3) inhibitors discovered by bioisosteric scaffold hopping approach, Eur J Med Chem, 139 (2017) 936-946.
[23] A.C. Pippione, F. Dosio, A. Ducime, A. Federico, K. Martina, S. Sainas, B. Frolund, M. Gooyit, K.D. Janda, D. Boschi, M.L. Lolli, Substituted 4-hydroxy-1,2,3-triazoles: synthesis, characterization and first drug design applications through bioisosteric modulation and scaffold hopping approaches, Medchemcomm, 6 (2015) 1285-1292.
[24] M.L. Lolli, S.L. Hansen, B. Rolando, B. Nielsen, P. Wellendorph, K. Madsen, O.M. Larsen, U. Kristiansen, R. Fruttero, A. Gasco, T.N. Johansen, Hydroxy-1,2,5-oxadiazolyl Moiety as Bioisoster of the Carboxy Function. Synthesis, Ionization Constants, and Pharmacological Characterization of γ-Aminobutyric Acid (GABA) Related Compounds, J Med Chem, 49 (2006) 4442-4446.
[25] M.L. Lolli, C. Giordano, D.S. Pickering, B. Rolando, K.B. Hansen, A. Foti, A. Contreras-Sanz, A. Amir, R. Fruttero, A. Gasco, B. Nielsen, T.N. Johansen, 4-Hydroxy-1,2,5-oxadiazol-3-yl Moiety as Bioisoster of the Carboxy Function. Synthesis, Ionization Constants, and Molecular Pharmacological Characterization at Ionotropic Glutamate Receptors of Compounds Related to Glutamate and Its Homologues, J Med Chem, 53 (2010) 4110-4118.
[26] S. Sainas, A.C. Pippione, M. Giorgis, E. Lupino, P. Goyal, C. Ramondetti, B. Buccinna, M. Piccinini, R.C. Braga, C.H. Andrade, M. Andersson, A.C. Moritzer, R. Friemann, S. Mensa, S. Al-Kadaraghi, D. Boschi, M.L. Lolli, Design, synthesis, biological evaluation and X-ray structural studies of potent human dihydroorotate dehydrogenase inhibitors based on hydroxylated azole scaffolds, Eur J Med Chem, 129 (2017) 287-302.
[27] M. Lolli, S. Narramore, C.W. Fishwick, K. Pors, Refining the chemical toolbox to be fit for educational and practical purpose for drug discovery in the 21st Century, Drug Discov Today, 20 (2015) 1018-1026.
[28] D. Ferraris, B. Duvall, Y.S. Ko, A.G. Thomas, C. Rojas, P. Majer, K. Hashimoto, T. Tsukamoto, Synthesis and biological evaluation of D-amino acid oxidase inhibitors, J Med Chem, 51 (2008) 3357-3359.
[29] M.C. Byrns, Y. Jin, T.M. Penning, Inhibitors of type 5 17beta-hydroxysteroid dehydrogenase (AKR1C3): overview and structural insights, J Steroid Biochem Mol Biol, 125 (2011) 95-104.
[30] C.M.M. Hendriks, T.M. Penning, T. Zang, D. Wiemuth, S. Gründer, I.A. Sanhueza, F. Schoenebeck, C. Bolm, Pentafluorosulfanyl-containing flufenamic acid analogs: Syntheses, properties and biological activities, Bioorg. Med. Chem. Lett., 25 (2015) 4437-4440.
[31] P.R. Savoie, J.T. Welch, Preparation and utility of organic pentafluorosulfanyl-containing compounds, Chem Rev, 115 (2015) 1130-1190.
[32] R. Gujjar, F. El Mazouni, K.L. White, J. White, S. Creason, D.M. Shackleford, X. Deng, W.N. Charman, I. Bathurst, J. Burrows, D.M. Floyd, D. Matthews, F.S. Buckner, S.A. Charman, M.A. Phillips, P.K. Rathod, Lead optimization of aryl and aralkyl amine-based triazolopyrimidine inhibitors of Plasmodium falciparum dihydroorotate dehydrogenase with antimalarial activity in mice, J Med Chem, 54 (2011) 3935-3949.
[33] S. Schrödinger Release 2018-1: QikProp, LLC, New York, NY, 2018, in.
[34] Y. Amano, T. Yamaguchi, T. Niimi, H. Sakashita, Structures of complexes of type 5 17β-hydroxysteroid dehydrogenase with structurally diverse inhibitors: insights into the conformational changes upon inhibitor binding, Acta Crystallogr., Sect. D: Biol. Crystallogr., 71 (2015) 918-927.
[35] http://www.rbvi.ucsf.edu/chimera, in.

[36] C. Zarantonello, A. Guerrato, E. Ugel, R. Bertani, F. Benetollo, R. Milani, A. Venzo, A. Zaggia, Synthesis and characterisation of 3- and 4-(pentafluorosulfanyl)benzoic acid derivatives. X-ray structure of 3-SF5-C6H4-COOH, Journal of Fluorine Chemistry, 128 (2007) 1449-1453.
[37] V. Vichai, K. Kirtikara, Sulforhodamine B colorimetric assay for cytotoxicity screening, Nat Protoc, 1 (2006) 1112-1116.
[38] E. Ugazio, L. Gastaldi, V. Brunella, D. Scalarone, S.A. Jadhav, S. Oliaro-Bosso, D. Zonari, G. Berlier, I. Miletto, S. Sapino, Thermoresponsive mesoporous silica nanoparticles as a carrier for skin delivery of quercetin, International Journal of Pharmaceutics, 511 (2016) 446-454.
[39] G.L. Gravina, A. Mancini, L. Scarsella, A. Colapietro, A. Jitariuc, F. Vitale, F. Marampon, E. Ricevuto, C. Festuccia, Dual PI3K/mTOR inhibitor, XL765 (SAR245409), shows superior effects to sole PI3K [XL147 (SAR245408)] or mTOR [rapamycin] inhibition in prostate cancer cell models, Tumour Biol, 37 (2016) 341-351.
[40] J. Komoto, T. Yamada, K. Watanabe, F. Takusagawa, Crystal Structure of Human Prostaglandin F Synthase (AKR1C3), Biochemistry, 43 (2004) 2188-2198.
[41] W. Kabsch, Automatic processing of rotation diffraction data from crystals of initially unknown symmetry and cell constants, J. Appl. Crystallogr., 26 (1993) 795-800.
[42] P.D. Adams, P.V. Afonine, G. Bunkoczi, V.B. Chen, I.W. Davis, N. Echols, J.J. Headd, L.-W. Hung, G.J. Kapral, R.W. Grosse-Kunstleve, A.J. McCoy, N.W. Moriarty, R. Oeffner, R.J. Read, D.C. Richardson, J.S. Richardson, T.C. Terwilliger, P.H. Zwart, PHENIX: a comprehensive Python-based system for macromolecular structure solution, Acta Crystallographica Section D, 66 (2010) 213-221.
[43] S. Schrödinger Release 2018-1: Glide, LLC, New York, NY, 2018, in.